

SACLANTCEN REPORT
serial no: SR-243

**SACLANT UNDERSEA
RESEARCH CENTRE
REPORT**



**SACLANT UNDERSEA RESEARCH CENTRE
LIBRARY COPY 1**

**ACOUSTIC BOTTOM CHARACTERIZATION
OF A SHALLOW WATER AREA
WEST OF MALLORCA**

*A. Caiti, F. Ingenito,
A. Kristensen, M.D. Max*

December 1995

The SACLANT Undersea Research Centre provides the Supreme Allied Commander Atlantic (SACLANT) with scientific and technical assistance under the terms of its NATO charter, which entered into force on 1 February 1963. Without prejudice to this main task – and under the policy direction of SACLANT – the Centre also renders scientific and technical assistance to the individual NATO nations.

This document is released to a NATO Government at the direction of SACLANT Undersea Research Centre subject to the following conditions:

- The recipient NATO Government agrees to use its best endeavours to ensure that the information herein disclosed, whether or not it bears a security classification, is not dealt with in any manner (a) contrary to the intent of the provisions of the Charter of the Centre, or (b) prejudicial to the rights of the owner thereof to obtain patent, copyright, or other like statutory protection therefor.
 - If the technical information was originally released to the Centre by a NATO Government subject to restrictions clearly marked on this document the recipient NATO Government agrees to use its best endeavours to abide by the terms of the restrictions so imposed by the releasing Government.
-

SACLANT Undersea Research Centre
Viale San Bartolomeo 400
19138 San Bartolomeo (SP), Italy

tel: +39-187-540.111
fax: +39-187-524.600

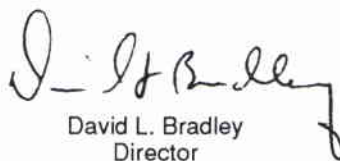
e-mail: library@saclantc.nato.int

SACLANTCEN SR-243

Acoustic bottom characterization of
a shallow water area west of
Mallorca

A. Caiti, F. Ingenito, A. Kristensen,
M. D. Max

The content of this document pertains to
work performed under Project 12 of the
SACLANTCEN Programme of Work.
The document has been approved for
release by The Director, SACLANTCEN.



David L. Bradley
Director

intentionally blank page

Acoustic bottom characterization of a shallow water area west of Mallorca

A. Caiti, F. Ingenito, A. Kristensen, M. D. Max

Executive Summary: Shallow water areas are becoming increasingly important as likely sites of naval operations. A requirement of sonar performance prediction models for shallow water is that they perform satisfactorily in the wide variety of environments normally found there. Transmission loss is the fundamental quantity for performance prediction, and of the environmental factors which affect transmission loss, the bottom is the most difficult to characterize. This report is part of a series which addresses bottom characterization and transmission loss prediction in representative shallow water areas.

The exercise was conducted in an area on the Balearic Shelf west of the island of Mallorca. The seafloor in this area is generally flat, with an impersistent veneer of sediment, no more than 4 m at its thickest, covering a hard limestone basement. The area was surveyed prior to the acoustic measurements using a high resolution seismic reflection boomer, a deeper penetrating seismic reflection sparker, and a side-scan sonar. The compressional velocity of the basement was measured by an acoustic inversion method and found to increase from 1970 m/s at the sediment-basement interface to 4305 m/s at a depth of 174 m. The shear velocity measurement technique allowed two possible interpretations, one yielding a shear velocity in the upper bottom layer of about 600 m/s and the other a shear velocity of about 1100 m/s. Transmission loss was measured using a four-element vertical array and explosive sources and processed in the 100–1600 Hz band.

Based on the environmental measurements, two geoacoustic models were constructed, one for each possible interpretation of the shear velocity data. These were used as input to the SAFARI transmission loss model to generate predictions for comparison with the transmission loss data. At high frequencies (400, 800, 1600 Hz) both geoacoustic models gave similar results, but at low frequencies (100, 200 Hz) the higher shear-velocity model gave better agreement with the measured transmission loss data. Therefore the high shear velocity model was accepted as a better description of the area.

The frequency of best propagation, or optimum frequency, was found to be about 800 Hz, higher than normally found in shallow water. This result, in agreement with theoretical predictions, is due to the high shear velocity which increases the loss at low frequencies. It suggests that in areas with hard, high shear-velocity bottoms, maximum detection range would be obtained at higher frequency than in areas with soft sedimentary bottoms



intentionally blank page



SACLANTCEN SR-243

Acoustic bottom characterization of a shallow water area west of Mallorca

A. Caiti, F. Ingenito, A. Kristensen, M. D. Max

Abstract: An experiment was conducted in shallow water on the Balearic Shelf west of the island of Mallorca. The seafloor in this area consists of a patchy layer of sediment less than 4 m thick overlying a hard limestone bottom. The compressional and shear velocities of the bottom were measured by remote sensing techniques using a geophone/hydrophone array deployed on the bottom and explosive sources. The compressional velocity in the basement was found to increase from 1970 m/s at the sediment-basement interface to 4305 m/s at a depth of 174 m. The shear velocity, determined from the inversion of interface wave data, was ambiguous, since there were two arrivals which could be interpreted as the interface wave. The slower arrival gave a shear velocity of about 600 m/s while the faster arrival gave a shear velocity of about 1100 m/s. Two geoacoustic models were constructed based on these results and used as inputs to SAFARI to predict transmission loss. Simultaneously with the bottom measurements, transmission loss was measured in a 100–1600 Hz band using explosive sources and a four element vertical array. At high frequencies (400, 800, 1600 Hz), in most cases, transmission loss predictions from both geoacoustic models compared reasonably well with the measurements, but at low frequencies (100, 200 Hz) the higher shear velocity model gave better agreement. The optimum frequency of propagation was about 800 Hz, higher than normally found in shallow water. This result is in agreement with theoretical predictions and is due to conversion to and subsequent absorption of shear waves in the bottom. It is suggested that the ambiguity in the determination of shear velocity could be due to anisotropy in the bottom.

Keywords: Balearic Shelf – bottom characteristics – Mallorca – shallow-water

Contents

1. Introduction	1
2. Geological description of the area	2
3. Experimental procedures.....	3
3.1. Bottom properties	3
3.2. Transmission loss measurements	3
4. Results of bottom measurements.....	5
4.1. Compressional velocity estimation.....	5
4.2. Shear velocity estimation	6
5. The geoacoustic model.....	8
6. Comparison of measured and predicted transmission loss.....	10
7. Optimum frequency.....	11
8. Conclusions	12
References.....	13
Annex A – Particle motion of interface wave arrivals	32

SACLANTCEN SR-243

1

Introduction

As part of its measurement programme, the Seafloor Acoustics Group conducted exercises in shallow-water areas selected to reflect the diversity of bottom types. To characterize an area, the acoustic properties of the bottom are measured employing standard SACLANTCEN techniques; the measured results, supplemented by acoustic parameters inferred from physical properties of the sediments, are used to construct a geoacoustic model of the bottom by the best fit method at a variety of frequencies. Transmission loss is measured over a broad frequency band simultaneously with the bottom measurements and compared with computations generated by a transmission loss model with the geoacoustic model as input. The degree of agreement between measured and calculated transmission loss serves as a test of the validity of the geoacoustic model.

Previously, we have reported on the results of an exercise in an area of the Adriatic with a silty-sand bottom [1] and two areas in the Strait of Sicily with hard sand bottom [2]. The subject of this report is an experiment conducted in March 1993 in shallow water on the Balearic Shelf west of the island of Mallorca, over a hard limestone bottom. We expected such a bottom to have a high shear velocity and, as a consequence, high transmission loss. This is due to the high shear velocity, but less than the sound velocity in the water column, energy is converted at the bottom interface into shear waves propagating in the bottom. The latter are highly attenuated, resulting in a decrease in the waterborne signal [3].

2

Geological description of the area

The Balearic Islands, comprising Menorca, Mallorca and Ibiza in the west, rest on a continental crustal fragment of the eastern Iberian Peninsula. The islands and their surrounding continental shelf form a prominent submarine peninsula eastward from the Spanish mainland in the otherwise deep water of the western Mediterranean. For at least the last five million years, since the Mediterranean flooded after the end-Messinian drying out when the sea passage to the Atlantic was closed, the shelf areas have been isolated from continental sediment supply, and no major rivers from the islands feed detrital sediments to the local continental shelf. Isolation from continental sediment in the relatively nutrient-poor Mediterranean has produced the sediment-starved Balearic shelves whose restricted sources of supply are Eolian material mainly African of origin, very restricted local erosion, and bioclastic material produced locally.

The experimental area is shown in Fig. 1. The seafloor in this area is generally flat. The acoustic basement occurs very near to, or at, the sea floor. Recent sediment cover, where it occurs, is present only as an impersistent thin veneer, with rare patches up to 4 m thick, except near the shelf edges where it rarely becomes as much as 20 m thick. There are large areas of exposed acoustic basement. The acoustic basement consists of a bedded series showing many parallel acoustic impedance horizons and an apparently unbedded type, which is acoustically transparent, with which well bedded slope sediments merge imperceptibly. This relationship suggests interbedding of limestones and off-reef limey muds and shales. The presence of reef knolls immediately beneath recent sediment cover at the margin of the plateau, the overall hardness of the acoustic basement, and internal bedding patterns that show draped bluffs and buried platforms, probably of a carbonate nature, strongly suggest that the platform surface beneath the thin recent sediment is composed of carbonate deposited on the shallow marine platform that existed when sea level began to rise after the last glacial event which ended about 11,000 years ago.

The area was surveyed immediately prior to the acoustic measurements using a high resolution seismic reflection boomer, a deeper penetrating seismic reflection sparker, and a side-scan sonar. The results of this investigation are reported in [4].

3.1. Bottom properties

In recent years the Seafloor Acoustics Group at SAACLANTCEN has developed several experimental techniques and data processing algorithms in order to estimate *in-situ* geoacoustic properties of the sea bottom. Most of the methodologies are based on the exploitation of seismic waves recorded with hydrophones and/or geophones on the seabed. A general discussion of the various types of waves and the information that can be retrieved from them can be found in [5]. The information from the seismic data is usually complemented with data from cores taken at the same sites, with bathymetric, side-scan sonar and shallow seismic surveys, and with geological information derived from the literature and from historical data-bases.

At the Mallorca site, the instrumentation deployed for the estimation of *in-situ* geoacoustic properties consisted of a hydrophone/geophone array (composed of ten geophones, sensitive to the vertical component of the particle velocity, spaced 5 m apart, plus three hydrophones, spaced 25 m apart) and two Ocean Bottom Seismometers (OBS), each one consisting of a tri-axial geophone and a hydrophone that were deployed near the array. The array was deployed on the bottom at the same location as the hydrophone array for the acoustic experiment. Very favourable weather conditions allowed for the deployment of the OBS very close (100 m) to the mid-part of the array. The OBS were equipped with tiltmeters and compasses in order to determine the exact orientation of the tri-axial geophones.

Small explosive charges were detonated at the sea bottom, end-fire to the array, on the same line as the acoustic experiment, at ranges of approximately 500 to 4000 m. Exact ranges were determined afterwards from the analysis of the recorded time series.

The additional information derived from cores and shallow seismic survey in the area indicates that the bottom is composed of a thin sand layer (with thickness varying between 0 and 4 m) overlying a consolidated structure that, from historical data, can be identified as limestone [4]. Both the seabed surface and the sand/limestone interface exhibit a rough character. Moreover, the side-scan sonar survey shows the presence in the area of outcropping rocks. However, the track for the seismic experiment was selected in order to minimize the effect of irregular scatterers.

3.2. Transmission loss measurements

The transmission loss track is shown in Fig. 2. A vertical hydrophone array with elements at depths 11, 21, 56, and 91 m was moored at point A and acted as the receiving array. The array was connected via a radio link to the NRV *Alliance* which dropped explosive charges approximately every kilometer along the track. The explosive charges were detonated at depths of 18 m and 90 m. The received signals

SACLANTCEN SR-243

were telemetered to the *Alliance* where they were recorded and subsequently processed in 1/3 octave bands to obtain transmission loss.

Results of bottom measurements

4.1. Compressional velocity estimation

Compressional velocity as a function of depth was estimated by analyzing the arrival time of the refracted wave (Fig. 3). From the arrival times as a function of range, compressional-wave velocity was estimated by use of the Wiechert-Herglotz-Bateman (WHB) inversion algorithm [5,6]. Since the ability of this technique to resolve the velocity of the uppermost sediment depends on the time of the arrival (i.e., the closer the range, the better the resolution), and since we do not have data at range close enough to resolve the first meters of sediment, constraints were put on the WHB method in order to have a compressional velocity of 1650 m/s at the seabed surface, as measured on cores taken during the exercise.

The WHB inversion method is based on the assumption of a continuous monotonically increasing compressional velocity profile with depth. The result is given through data points that should ideally be connected with a smooth continuous curve. However, to facilitate the modelling part, we present the results in terms of discretized layers, with constant compressional velocity in each layer.

The results of the WHB inversion are given in Table 1. They are consistent values reported for limestone [7] in the literature.

Table 1 *Compressional velocity C_p vs depth as estimated from the refraction analysis*

Depth (m)	C_p (m/s)
0.0	1650
4.0	1970
13.0	2273
24.5	2560
38.0	2830
54.0	3084
71.0	3323
90.0	3547
110.0	3757
130.5	3953
152.0	4135
174.0	4305

4.2. Shear velocity estimation

Shear velocity as a function of depth was estimated by the inversion of the group velocity of the interface wave travelling at the water-bottom boundary, with an algorithm described in detail in [8]. The interface wave is usually the low-frequency late arrival in the recorded time series. An arrival with these characteristics could be consistently identified in the time series recorded by the vertical geophones. The group velocity was determined by the multiple-filter analysis of the part of the signal identified as the interface wave. The result of the multiple-filter analysis was presented as a contour plot of signal energy as a function-of-frequency – and velocity-j usually referred to as a Gabor diagram. The group velocity was identified as the ridge crest of the Gabor diagram. Gabor diagrams of different signals were stacked in order to get a mean group velocity, and also to assess data variability.

In Fig. 4 a typical Gabor diagram of the late arrival is shown. The inversion results on the group velocity of this late arrival are given in Table 2.

Table 2 Shear velocity C_s vs depth as estimated from the interface wave inversion of the late arrival

Depth (m)	C_s (m/s)
0.0	582
10.0	652
20.0	682
30.0	679
45.0	771
60.0	959

Two comments need to be made. The first is that, with the group velocity available at frequencies below 10 Hz, the inversion method was not able to resolve shear wave velocity structure at intervals in depth less than 10 m. The second, more critical, observation is that the estimated shear-velocity values seem too low when compared with the estimated compressional velocities. For instance, the ratio of the compressional velocity to the shear velocity at 30 m depth is approximately 3.8. This is much higher than the typical ratio for limestone [7] of 1.9, and also higher than the ratios for other consolidated sediments and rocks.

In some of the longest range shots, it was possible to identify another low frequency group arrival at a velocity of about 1000 m/s. When multiple-filter analysis was applied, a Gabor diagram similar to the one shown in Fig. 5 was obtained. This resembles the Gabor diagram of a dispersive interface wave; however, since the frequency range is between 6 and 9 Hz, we have too few group velocity data points to make a complete inversion for shear velocity as a function of depth. For the discussion here, it is sufficient to say that, if the low frequency arrival is an interface wave, its velocity would approximately correspond to an average shear velocity of 1100 m/s in the first 75 m of sediment (using a 0.9 value for the interface wave/shear-wave velocity ratio, and a penetration in the bottom of about half a wavelength). This shear velocity value would be in much better agreement with limestone or with other consolidated bottom types.

SACLANTCEN SR-243

In an attempt to determine which of the two arrivals is the interface wave, we investigated the particle motion as recorded by the tri-axial OBS, but the results were inconclusive. Details of the particle motion study are given in Annex A.

5

The geoacoustic model

A geoacoustic model was constructed for the area near the array site based on Tables 1 and 2. The model is shown in Table 3. The sound-velocity profile in the water column was obtained from a CTD cast taken at the array site at the time of the transmission loss measurement. The points in Tables 1 and 2 were used to generate smooth velocity profiles which were approximated by a series of layers, with constant environmental parameters in each layer, as required by the SAFARI transmission loss model. In Table 3 the depth given is the depth of the top of a layer and the parameters given are constant throughout the layer.

Table 3 *The geoacoustic model based on compressional velocities C_p and shear velocities C_s of Tables 1 and 2*

Depth (m)	C_p (m/s)	C_s (m/s)	α_p (dB/ λ)*	α_s (dB/ λ)*
0.0	1506.4	0.0	0.0	0.0
40.0	1506.4	0.0	0.0	0.0
59.0	1508.4	0.0	0.0	0.0
109.0	1650.0	80.0	1.2	2.6
110.0	2160.0	650.0	0.056	0.015
120.0	2405.0	670.0	0.061	0.016
130.0	2605.0	690.0	0.065	0.017
140.0	2850.0	695.0	0.070	0.017
155.0	3080.0	775.0	0.074	0.019
170.0	3300.0	830.0	0.078	0.023
185.0	3480.0	960.0	0.082	0.024
200.0	3620.0	1100.0	0.084	0.026
210.0	5500.0	3000.0	0.110	0.060

*The compressional and shear attenuations are taken from Hamilton [9].

The shear velocity in the sediment layer and the compressional and shear attenuation were taken from Hamilton [9], where the sediment layer was taken to be silty-sand and the subbottom limestone. The above geoacoustic model, when used as input to SAFARI, gave poor results in comparison with the measured low frequency transmission loss (see below). Therefore a second geoacoustic model was developed using, instead of the shear profile of Table 2, shear velocities and attenuations calculated by assuming the compressional to shear velocity ratio of 1.9. This model is given in Table 4.

SACLANTCEN SR-243

Table 4 *The geoacoustic model based on compressional velocities C_p from Table 1 and shear velocities C_s obtained by taking C_p/C_s to be 1.9*

Depth (m)	C_p (m/s)	C_s (m/s)	α_p (dB/ λ)*	α_s (dB/ λ)*
0.0	1506.4	0.0	0.0	0.0
40.0	1506.4	0.0	0.0	0.0
59.0	1508.4	0.0	0.0	0.0
109.0	1650.0	80.0	1.2	2.6
110.0	2160.0	1140.0	0.056	0.029
120.0	2405.0	1270.0	0.061	0.032
130.0	2605.0	1370.0	0.065	0.034
140.0	2850.0	1500.0	0.070	0.037
155.0	3080.0	1620.0	0.074	0.039
170.0	3300.0	1740.0	0.078	0.041
185.0	3480.0	1830.0	0.082	0.043
200.0	3620.0	1900.0	0.084	0.044
210.0	5500.0	3000.0	0.110	0.060

*The compressional and shear attenuations are taken from Hamilton [9].

6

Comparison of measured and predicted transmission loss

The geoacoustic models of Tables 3 and 4 were each used as input to the SAFARI model to predict transmission loss for comparison with the measured data. Comparisons were made at 100, 200, 400, 80 and 1600 Hz for the source depths of 18 m and 90 m and receiver depths of 11, 21, 56 and 91 m. The results are shown in Figs. 6–45, where the circles are the measured data, the solid lines are the SAFARI predictions using the geophysical model of Table 4 as input and the dotted lines are the SAFARI predictions using the geophysical model of Table 3 as input. It can be seen that for 400 Hz and above there is very little difference between the predictions of the two models. At 100 and 200 Hz, however, the differences are dramatic, with the high shear velocity model giving 20 to 25 dB more loss at the longest range than the low shear model. In general, the agreement between the measured data and the high shear velocity model is satisfactory, except for a few disturbing cases, such as the 18 m source and the 91 m receiver.

A number of variations on the high shear velocity model were tried to improve the fit:

- a) The thickness of the sediment was varied. This had no effect on the transmission loss at low frequencies, the major region of discrepancy.
- b) Attenuations in both the sediment layer and the bottom were increased, with little effect on the transmission loss. The major contributor to the transmission loss is the high shear velocity in the bottom.
- c) Since there was a change in water depth over the measurement track, the coupled SNAP transmission loss model was run for a number of cases using the range dependent bathymetry measured on the depth sounder. No significant difference was found between range-independent and coupled SNAP results.

7

Optimum frequency

A characteristic of shallow-water propagation is the existence of a frequency of minimum transmission loss, or optimum frequency, which depends on the environment and on the source and receiver depths. The optimum frequency is often determined by replotting the data as contours of transmission loss *versus* frequency and range (Figs. 46–53) although a distinct optimum frequency is not always evident. In Fig. 47, for example, the optimum frequency, as indicated by the minimum of the 70 dB contour, lies between 800 and 1600 Hz. The optimum frequency is more difficult to determine for some of the other source–receiver combinations but appears to be in the neighborhood of 800 Hz in most cases. This is higher than is normally found in shallow water. According to the theoretical study of Jensen and Kuperman [10] the optimum frequency should be primarily dependent on the water depth and secondarily on the sound-velocity profile. For the conditions prevailing at the Mallorca site they predict an optimum frequency of about 200 Hz. However, Jensen and Kuperman also predict that the presence of a shear supporting bottom will increase the optimum frequency due to the increased loss at lower frequencies, caused by the conversion to and subsequent absorption of shear waves in the bottom. Hence, the present data can be taken as a confirmation of their prediction.

8

Conclusions

It appears that the measured low-frequency transmission loss at the Mallorca site cannot be accounted for other than by the assumption of a high shear velocity in the bottom. High shear velocity is also consistent with the measured compressional velocity. Generally satisfactory agreement between measured and predicted loss was obtained over the frequency band 100–1600 Hz except for a few cases. In judging the quality of the agreement between the measured and predicted transmission loss, it should be kept in mind that the geoacoustic model of the area was constructed as nearly as possible from independent measurements of the bottom parameters, with no fitting of the data attempted.

If one accepts the high shear velocity as correct, it follows that the late arrival observed on the geophones is not the interface wave (see Annex A). Further analysis, based on the particle motion, has failed to elucidate the nature of the late arrival, and further experimental work, along the lines suggested in Annex A, appears to be necessary.

References

-
- [1] Akal, T., Caiti, A., Curzi, P., Ingenito, F., Kristensen, A., Richardson, M., and Stoll, R. A test of bottom parameterization techniques in the Adriatic Sea. (SACLANTCEN Report, in preparation).
 - [2] Caiti, A., Ingenito, F., Kristensen, A., and Max, M. D. Measurements of bottom parameters and transmission loss at two sites in the Strait of Sicily. (SACLANTCEN Report, in preparation).
 - [3] Ingenito, F. and Wolf, S. N. Acoustic propagation in shallow water overlying a consolidated bottom. *Journal of the Acoustical Society of America*, **60**, 1976: 611–617.
 - [4] Max, M.D., Michelozzi, E., Tonarelli, B., Turgutcan, F. Shallow seafloor geology and sediment character of the western Mallorca Platform. (SACLANTCEN Report, in preparation).
 - [5] Akal, T., Caiti, A., and Stoll, R.D. Remote sensing in shallow-water marine sediments. *Proceedings of the Institute of Acoustics*, **15**, 1993: 221–228.
 - [6] Aki, K. and Richards, P.G. *Quantitative Seismology*, volume 2. San Francisco, W. H. Freeman, 1980, p. 643 [ISBN 071-6710595]
 - [7] Hamilton, E.L. V_p/V_s and Poisson ratios in marine sediments and rocks. *Journal of the Acoustical Society of America*, **66**, 1979: 1093–1101
 - [8] Caiti, A., Akal, T. and Stoll, R. D. Estimation of shear wave velocities in shallow marine sediments. *IEEE Journal of Oceanic Engineering*, **19**, 1994: 58–72.
 - [9] Hamilton, E. L. Acoustic properties of sediments, *In: Lara-Saenz, A., Ranz-Guerra, C., Carbo-Fite, C. eds. Acoustics and Ocean Bottom*, Madrid, C.S.I.C., 1987 [ISBN 84-00-06553-0]
 - [10] Jensen, F.B. and Kuperman, W.A. Optimum frequency of propagation in shallow water environments. *Journal of the Acoustical Society of America*, **73**, 1983: 813–819.
 - [11] Macbeth, C. Shear wave anisotropy in marine sediments around Britain from surface sources, *In: Hovem, J.M., Richardson, M.D., and Stoll, R.D. eds. Shear Waves in Marine Sediments*. Dordrecht, Kluwer, 1991: pp.195–202 [ISBN 0-7923-1357-7]
 - [12] Snoek, M. and Rauch, D. Spatial variability in ground motion: effects of material heterogeneity in seafloor sediments, *In: Hovem, J.M., Richardson, M.D., and Stoll, R.D. eds. Shear Waves in Marine Sediments*. Dordrecht, Kluwer, 1991: pp.213–219 [ISBN 0-7923-1357-7]

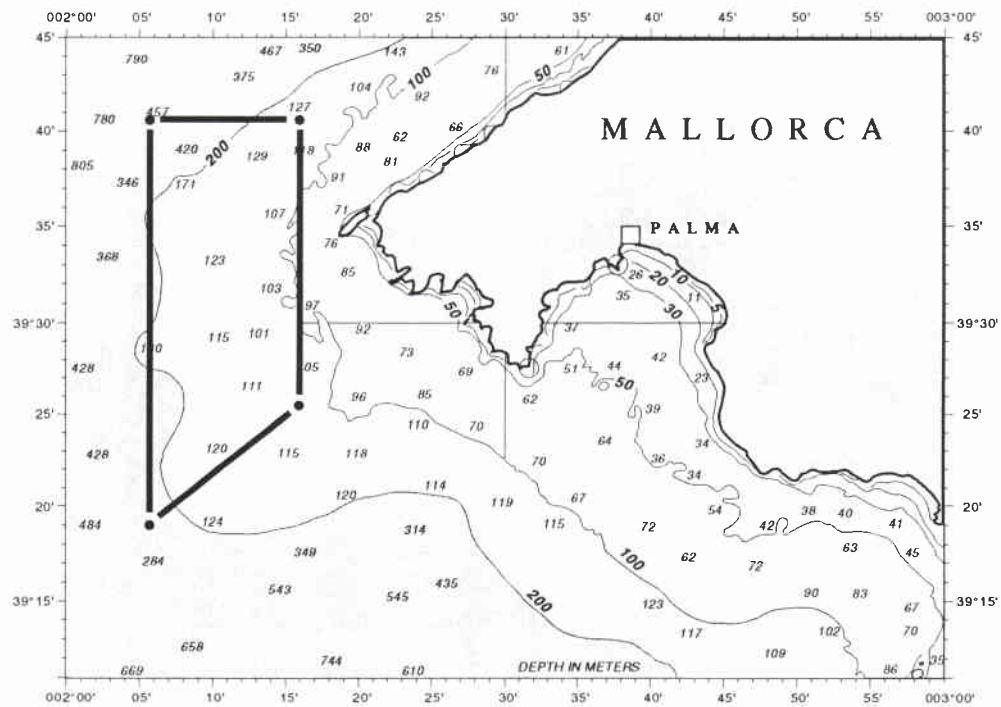


Figure 1 The Balearic shelf west of Mallorca. The experimental area is outlined by the dark lines.

SACLANTCEN SR-243

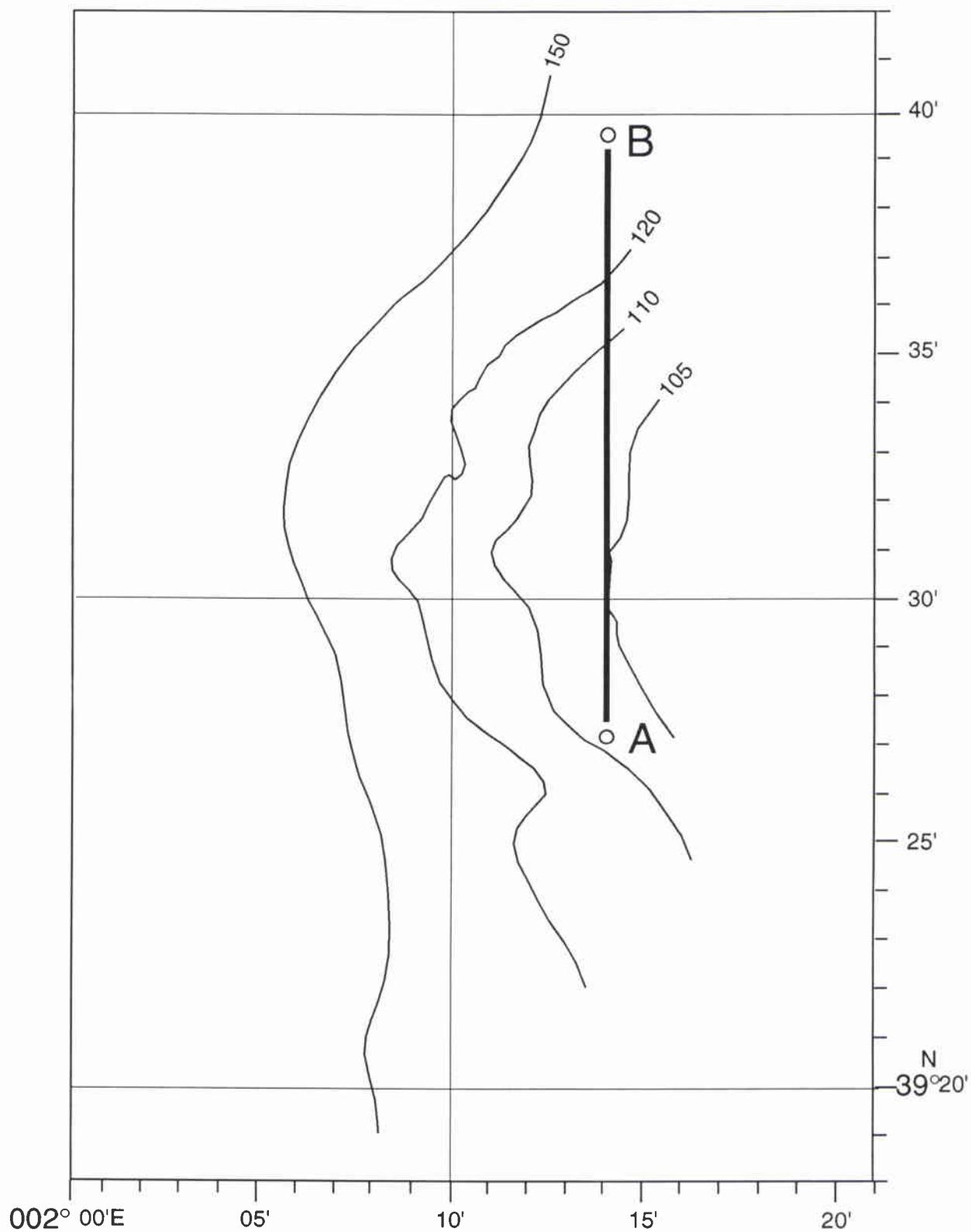


Figure 2 Transmission loss track A-B with the receiving array at A. Depths are in metres.

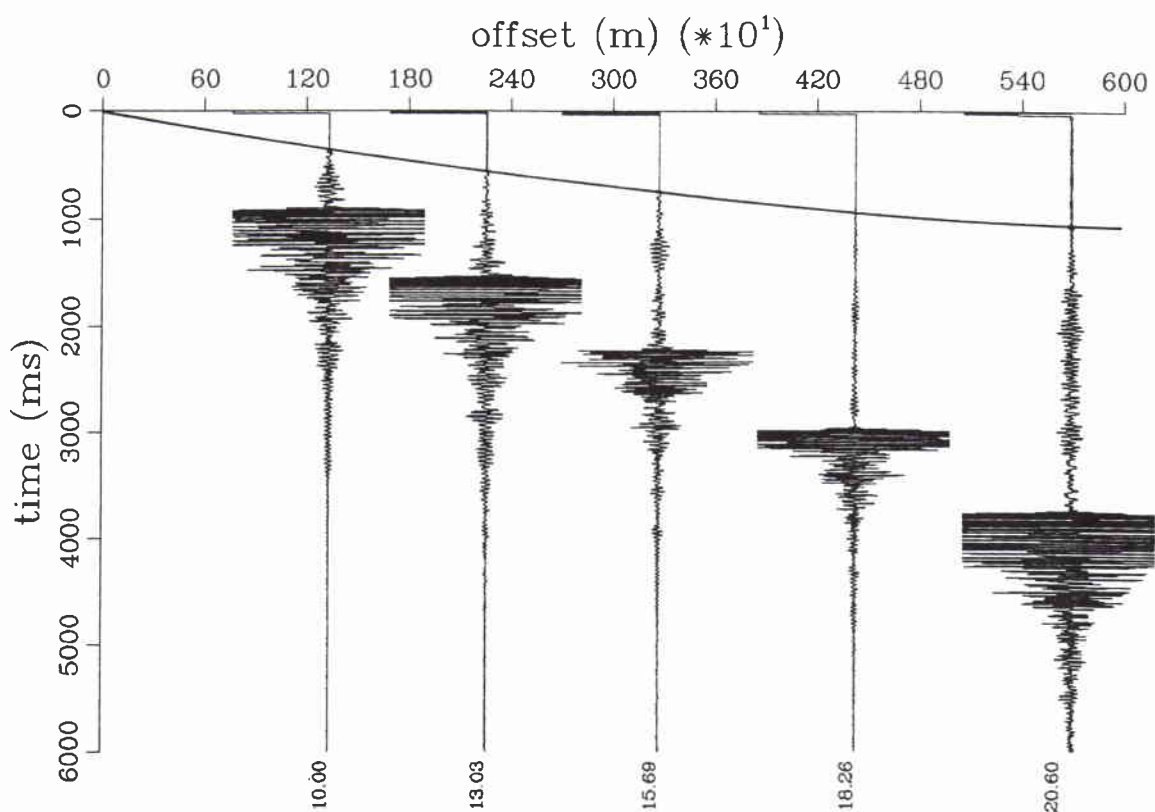


Figure 3 Arrival time vs. range as measured on the geophone array. The line connects the first refracted arrival.

SACLANTCEN SR-243

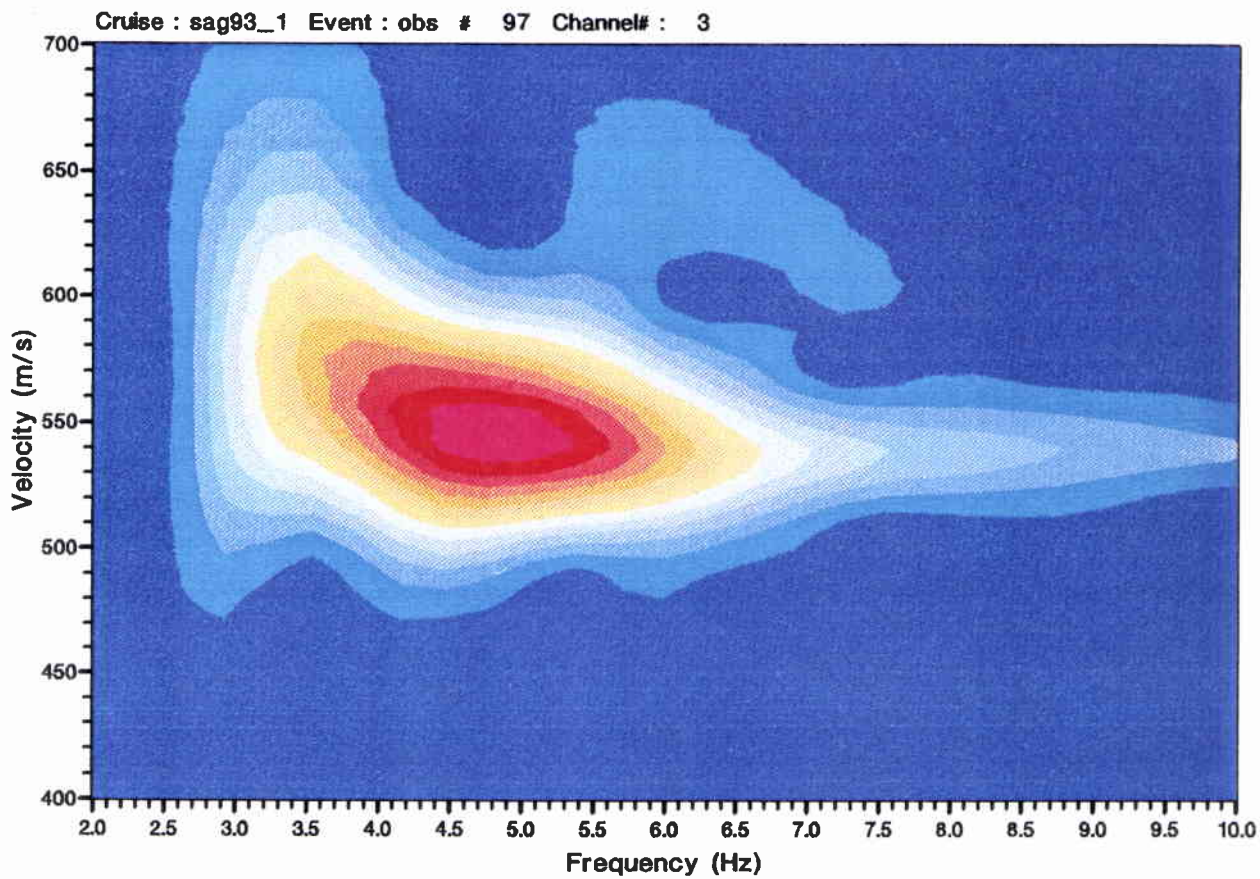
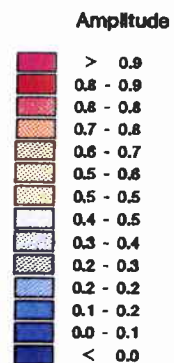


Figure 4 Gabor diagram of the late, low-frequency arrival.



intentionally blank page

SACLANTCEN SR-243

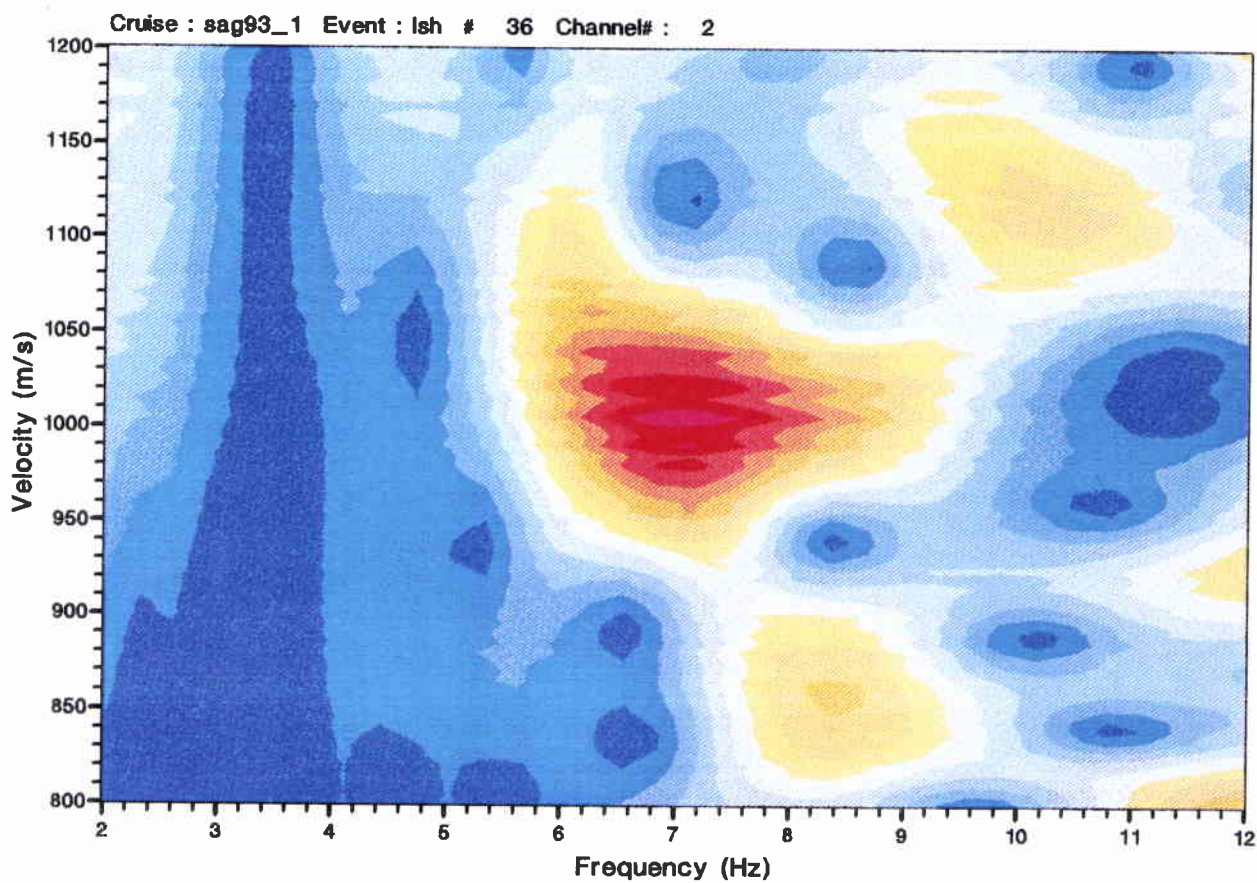
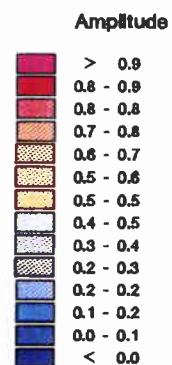
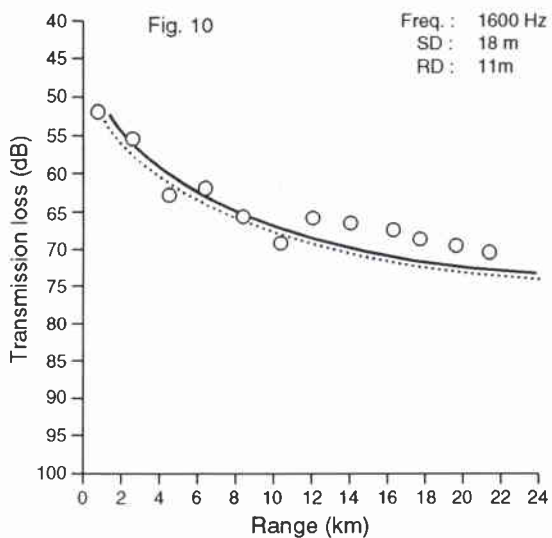
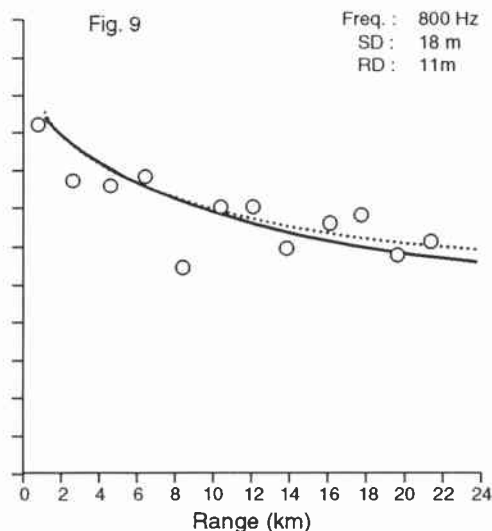
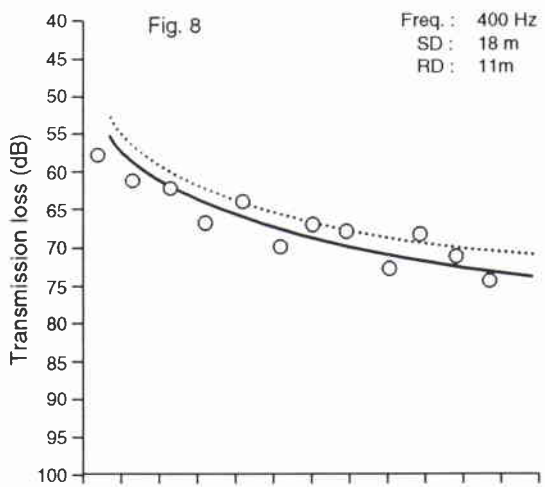
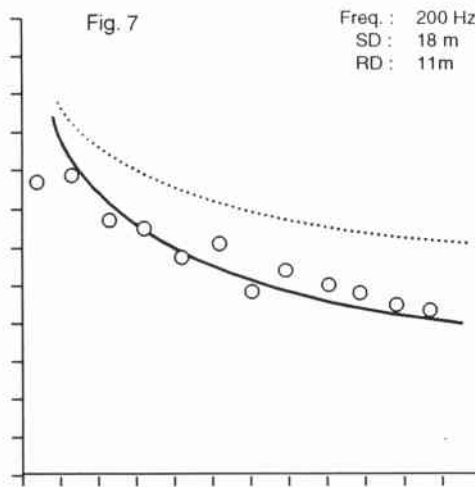
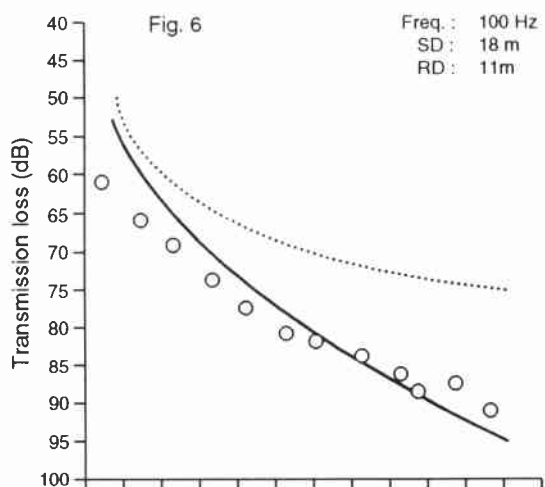


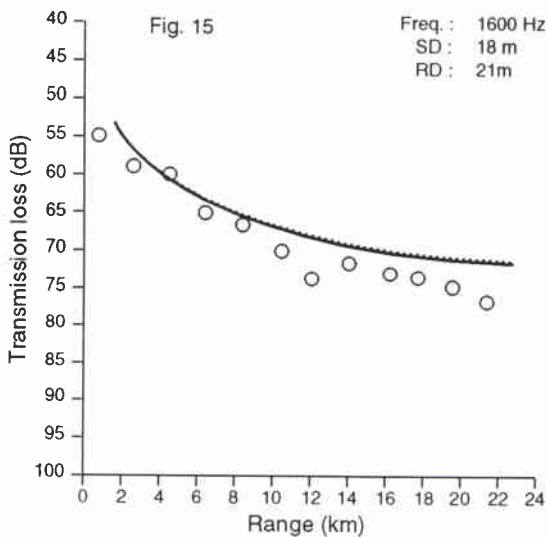
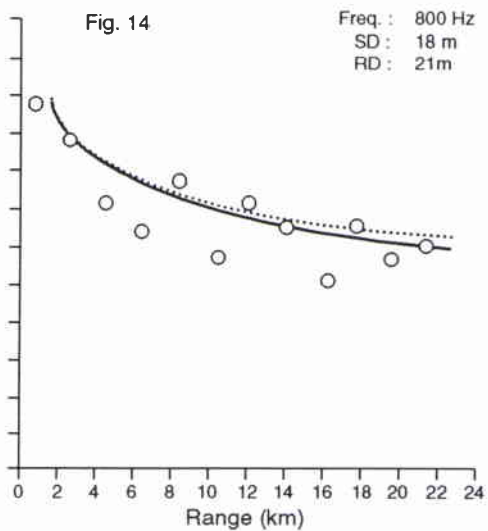
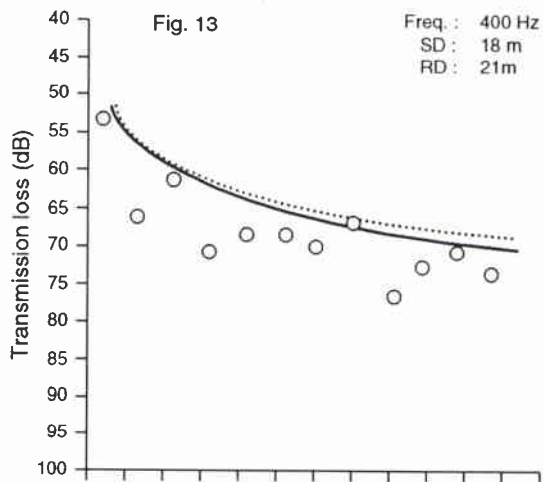
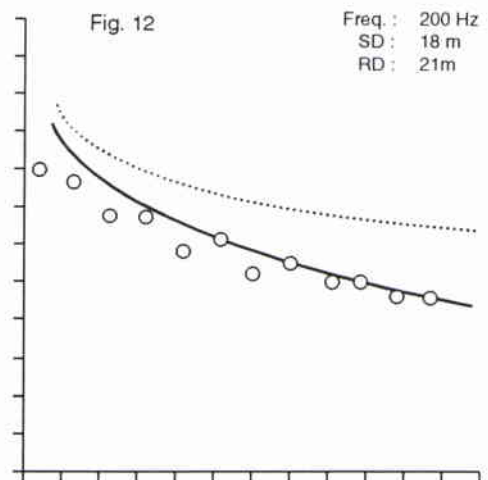
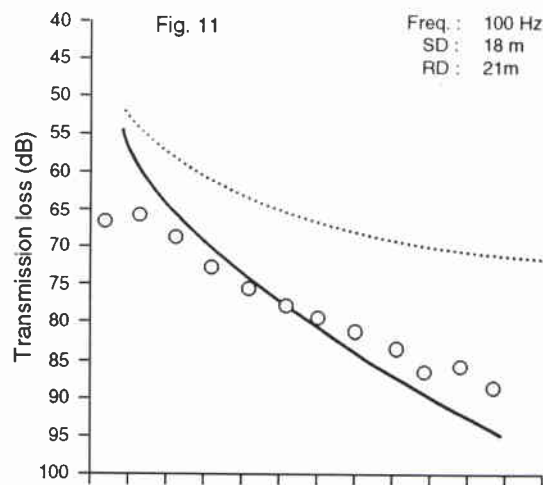
Figure 5 Gabor diagram of the high-velocity, low-frequency arrival.



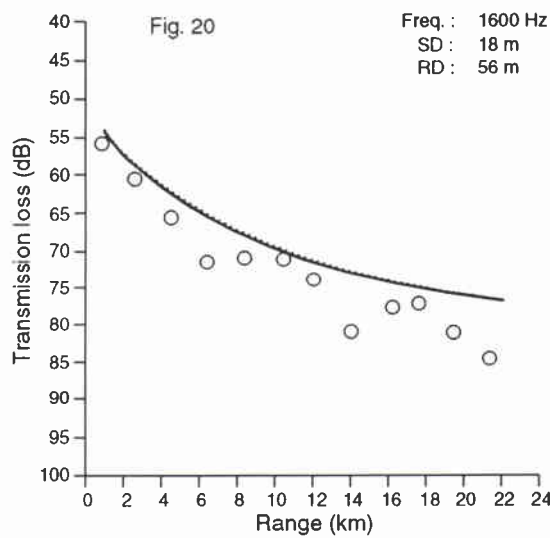
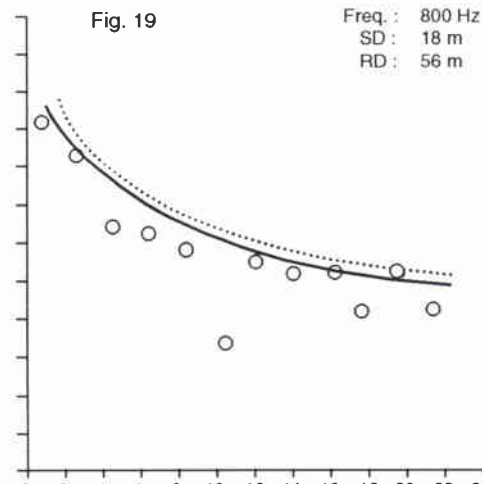
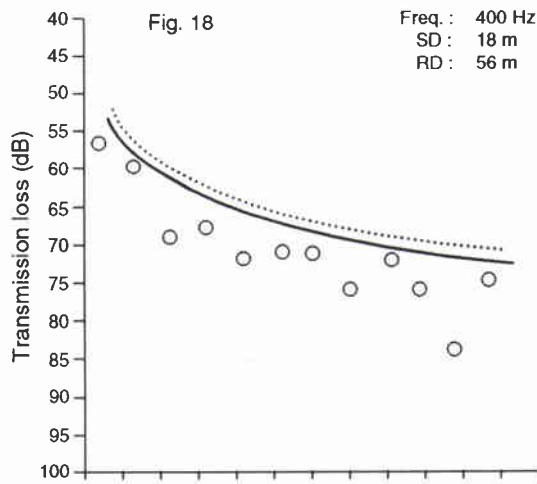
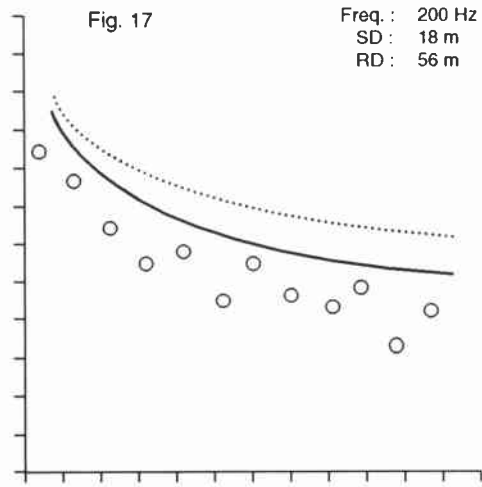
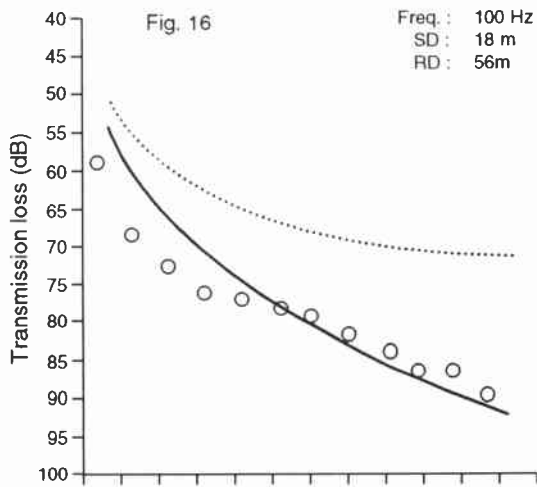


Figures 6–10 Transmission loss vs range. The circles are the measurements, processed in a 1/3 octave band. The solid line the SAFARI prediction using the high shear-velocity geoacoustic model of Table 4, while the dotted line is the SAFARI prediction using the low shear-velocity model of Table 3. SD=18 m; RD=11 m

SACLANTCEN SR-243

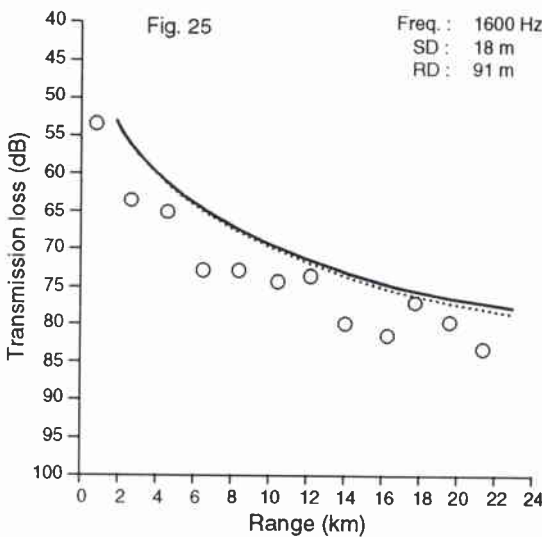
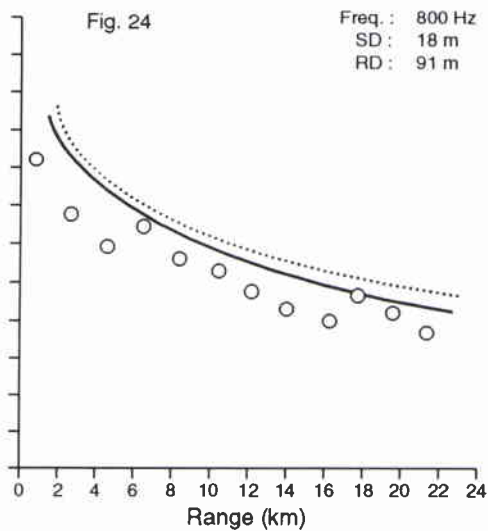
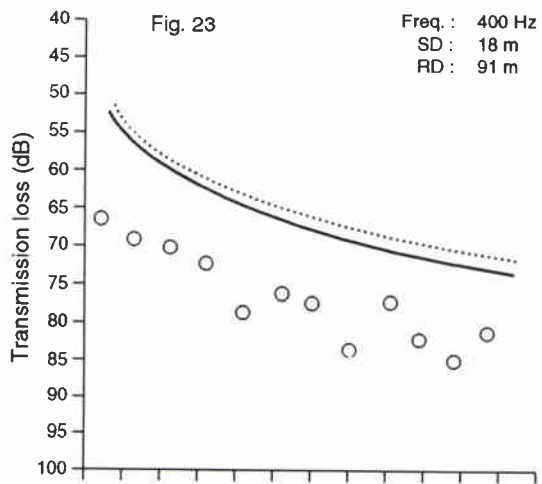
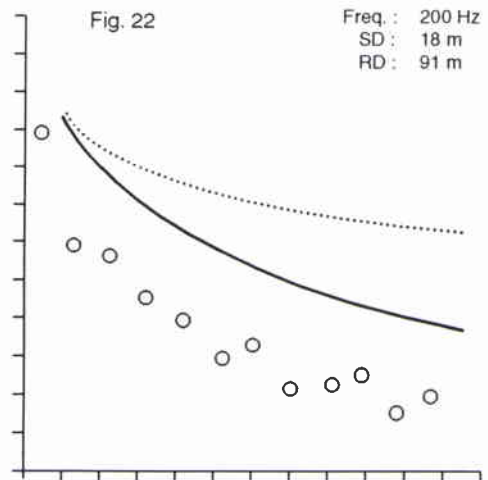
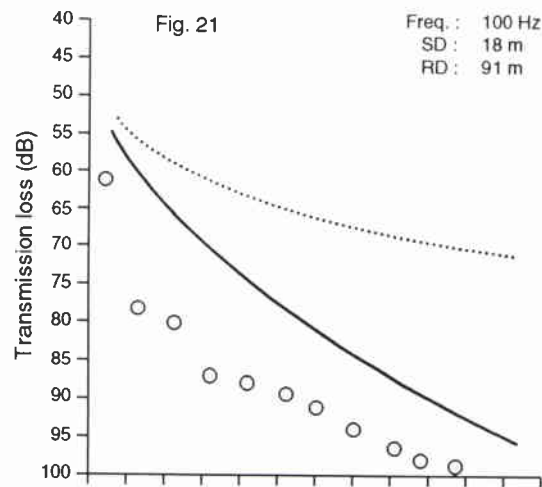


Figures 11–15 Transmission loss vs range. The circles are the measurements, processed in a 1/3 octave band. The solid line the SAFARI prediction using the high shear-velocity geoacoustic model of Table 4, while the dotted line is the SAFARI prediction using the low shear-velocity model of Table 3. SD=18 m; RD=21 m

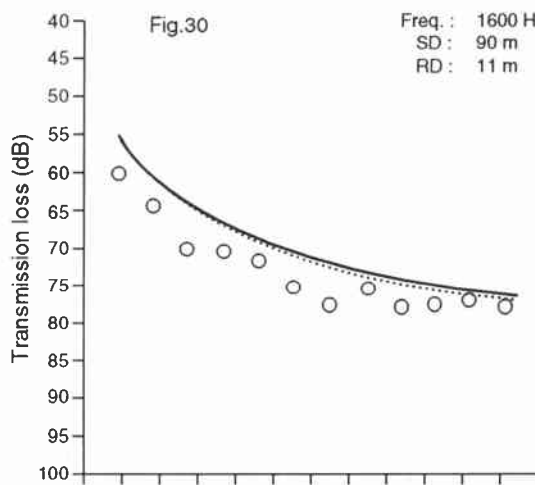
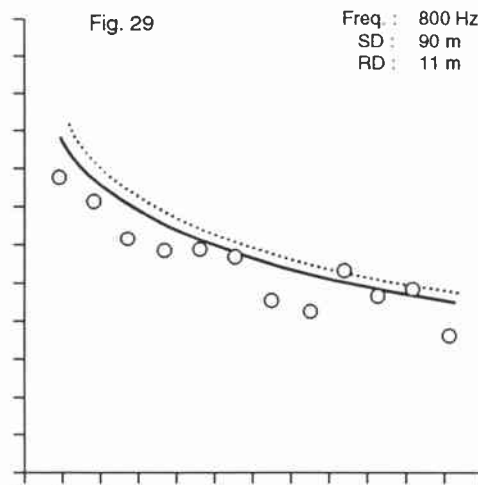
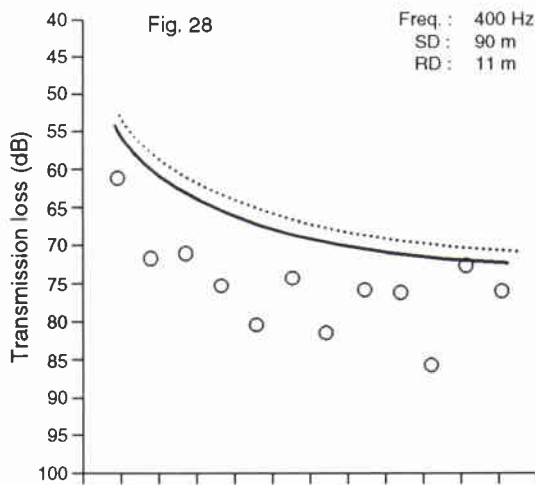
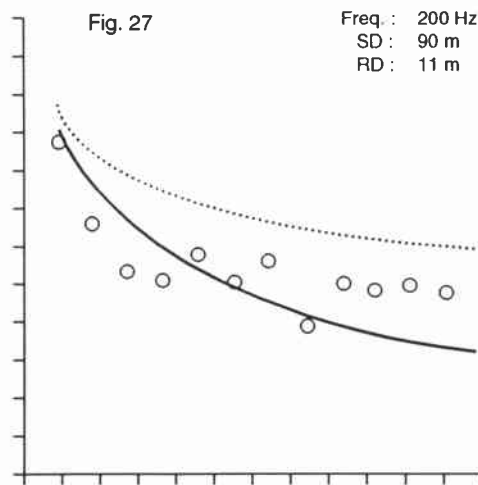
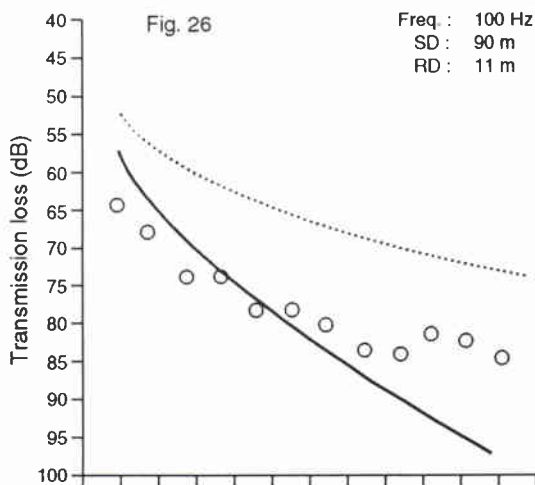


Figures 16–20 *Transmission loss vs range. The circles are the measurements, processed in a 1/3 octave band. The solid line the SAFARI prediction using the high shear-velocity geoacoustic model of Table 4, while the dotted line is the SAFARI prediction using the low shear-velocity model of Table 3. SD=18 m; RD=56 m*

SACLANTCEN SR-243

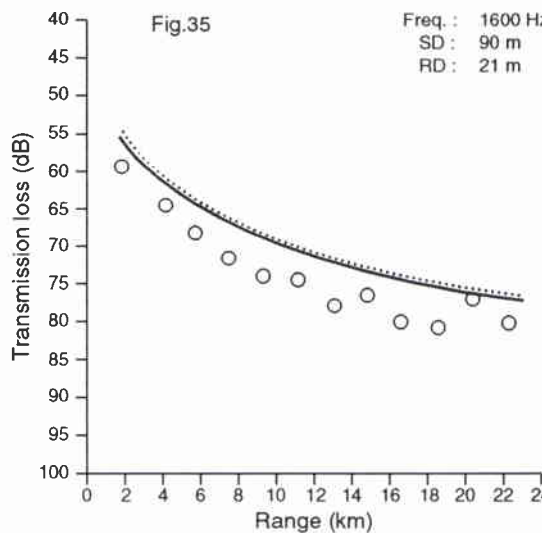
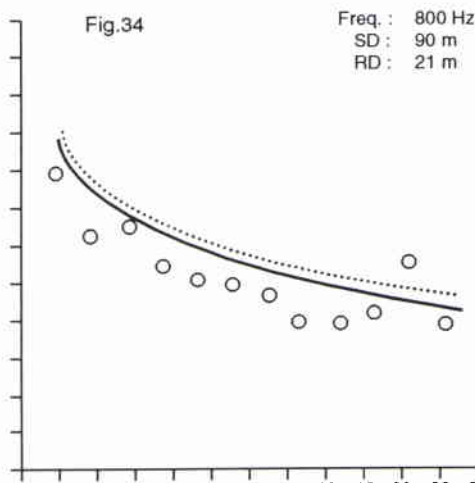
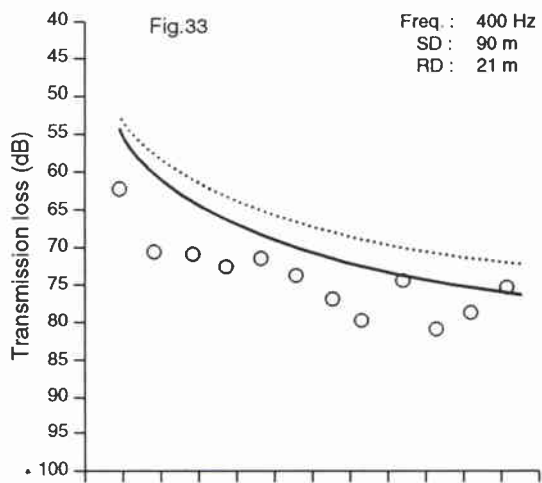
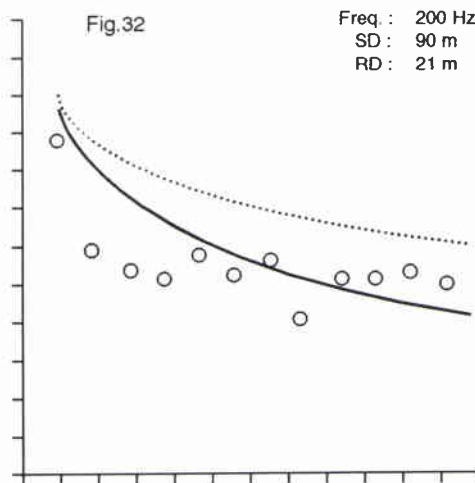
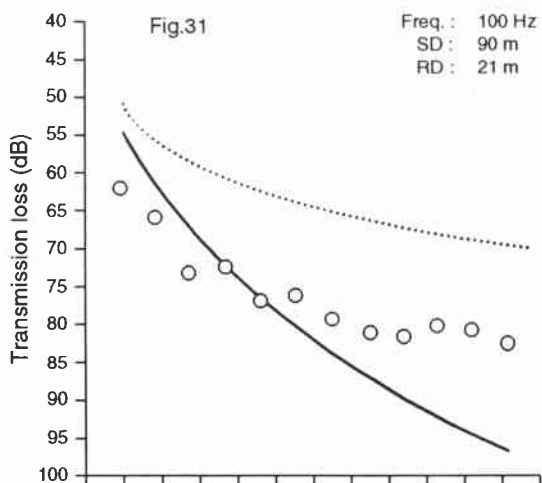


Figures 21–25 *Transmission loss vs range.* The circles are the measurements, processed in a 1/3 octave band. The solid line the SAFARI prediction using the high shear-velocity geoacoustic model of Table 4, while the dotted line is the SAFARI prediction using the low shear-velocity model of Table 3. SD=18 m; RD=91 m

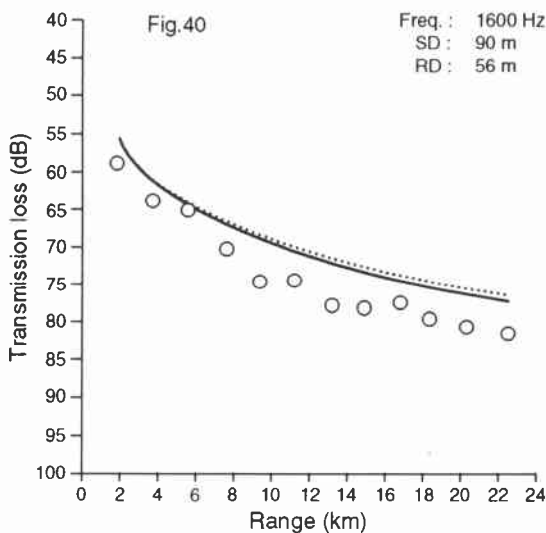
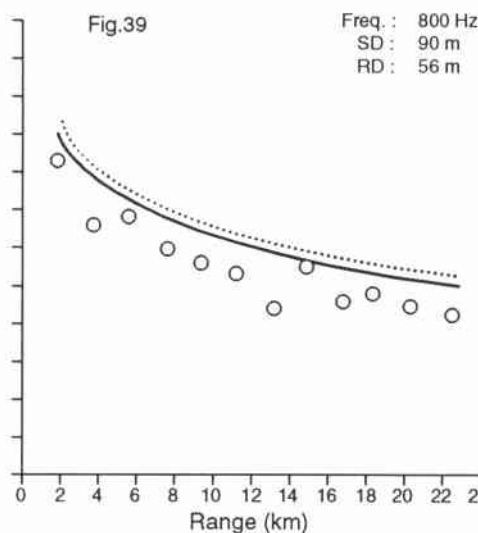
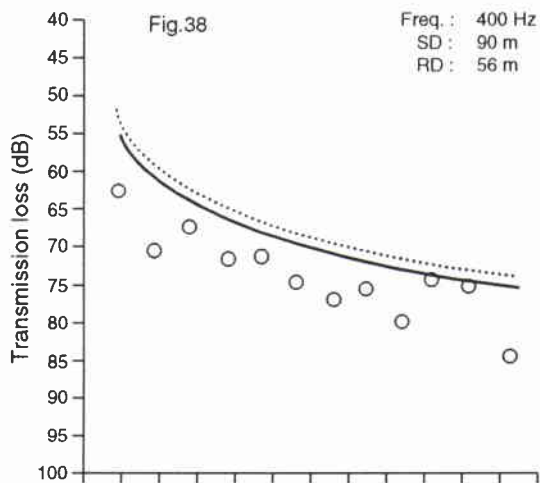
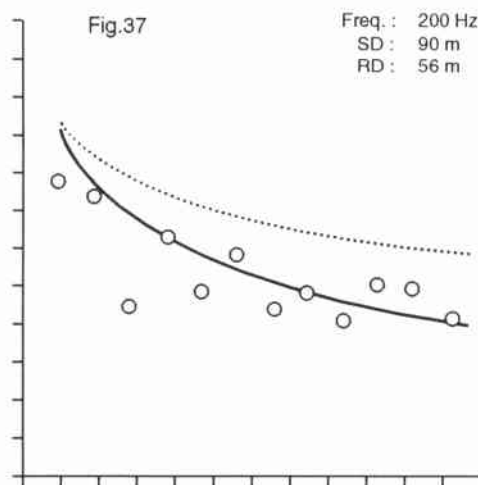
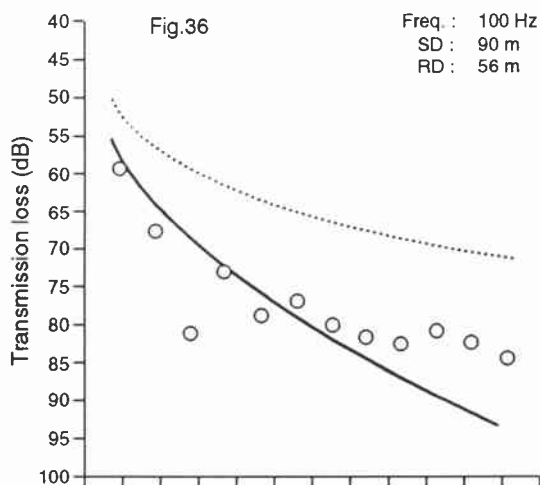


Figures 26–30 Transmission loss vs range. The circles are the measurements, processed in a 1/3 octave band. The solid line the SAFARI prediction using the high shear-velocity geoacoustic model of Table 4, while the dotted line is the SAFARI prediction using the low shear-velocity model of Table 3. SD=90 m; RD=11 m

SACLANTCEN SR-243

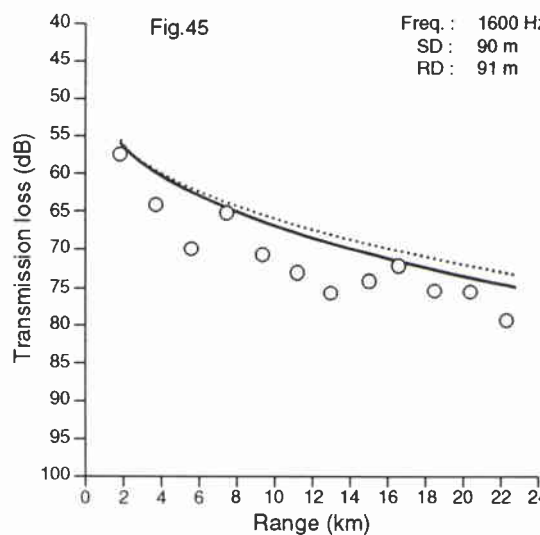
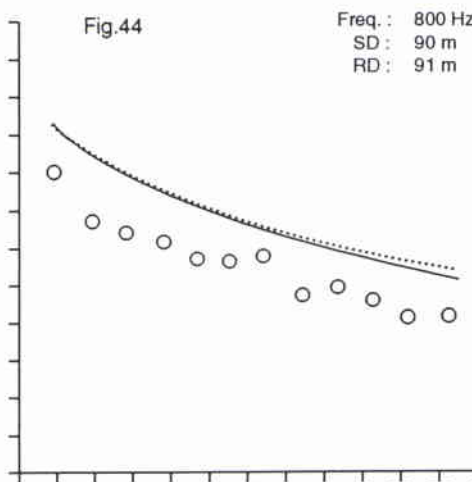
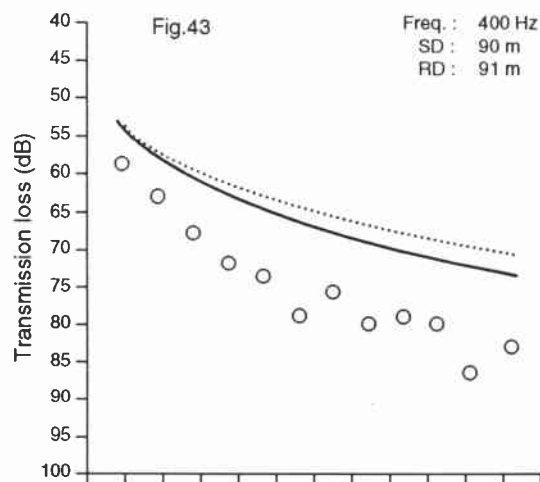
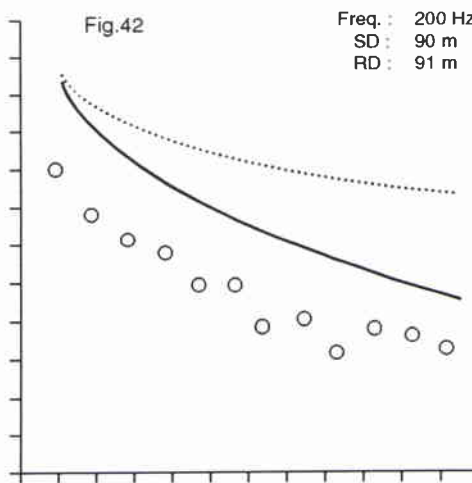
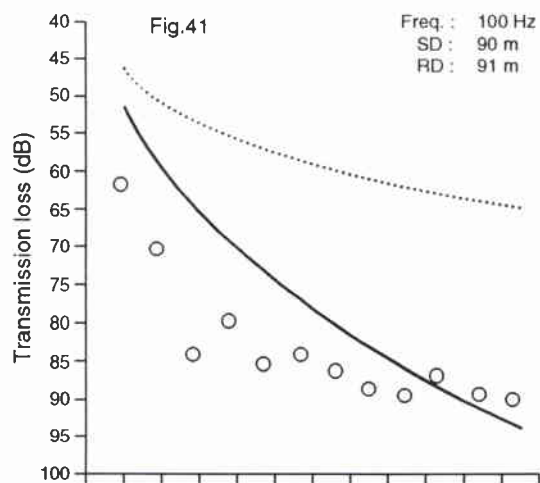


Figures 31–35 Transmission loss vs range. The circles are the measurements, processed in a 1/3 octave band. The solid line the SAFARI prediction using the high shear-velocity geoacoustic model of Table 4, while the dotted line is the SAFARI prediction using the low shear-velocity model of Table 3. SD=90 m; RD=21 m

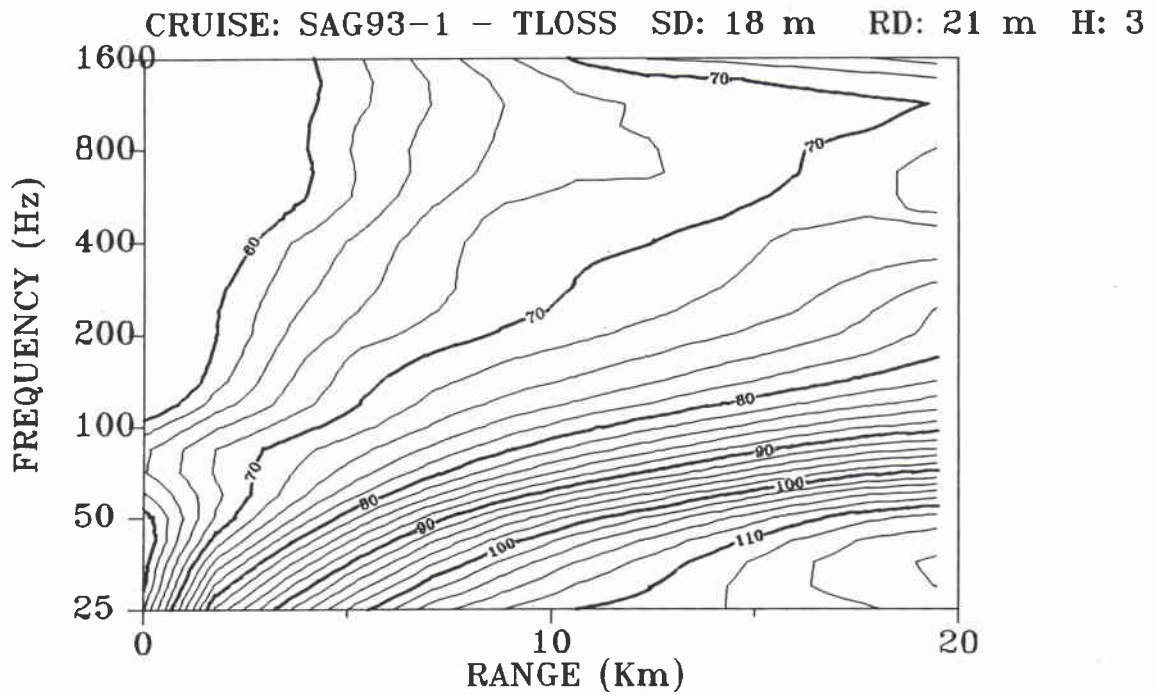
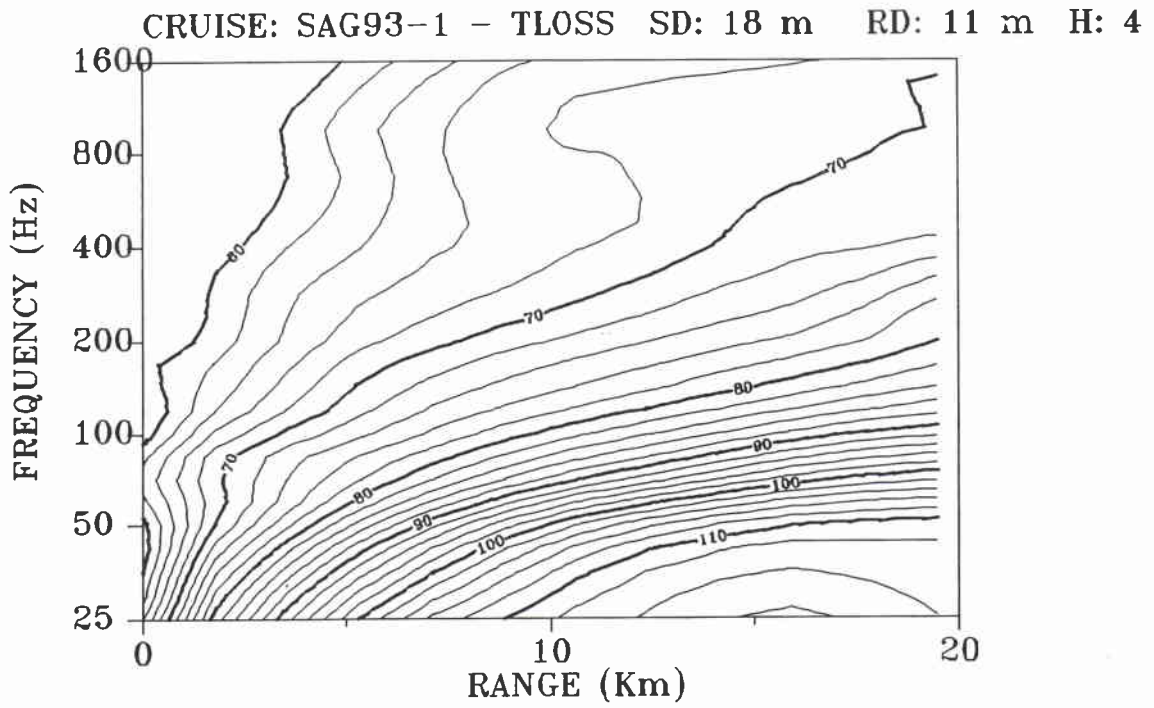


Figures 36–40 Transmission loss vs range. The circles are the measurements, processed in a 1/3 octave band. The solid line the SAFARI prediction using the high shear-velocity geoacoustic model of Table 4, while the dotted line is the SAFARI prediction using the low shear-velocity model of Table 3. SD=90 m; RD=56 m

SACLANTCEN SR-243

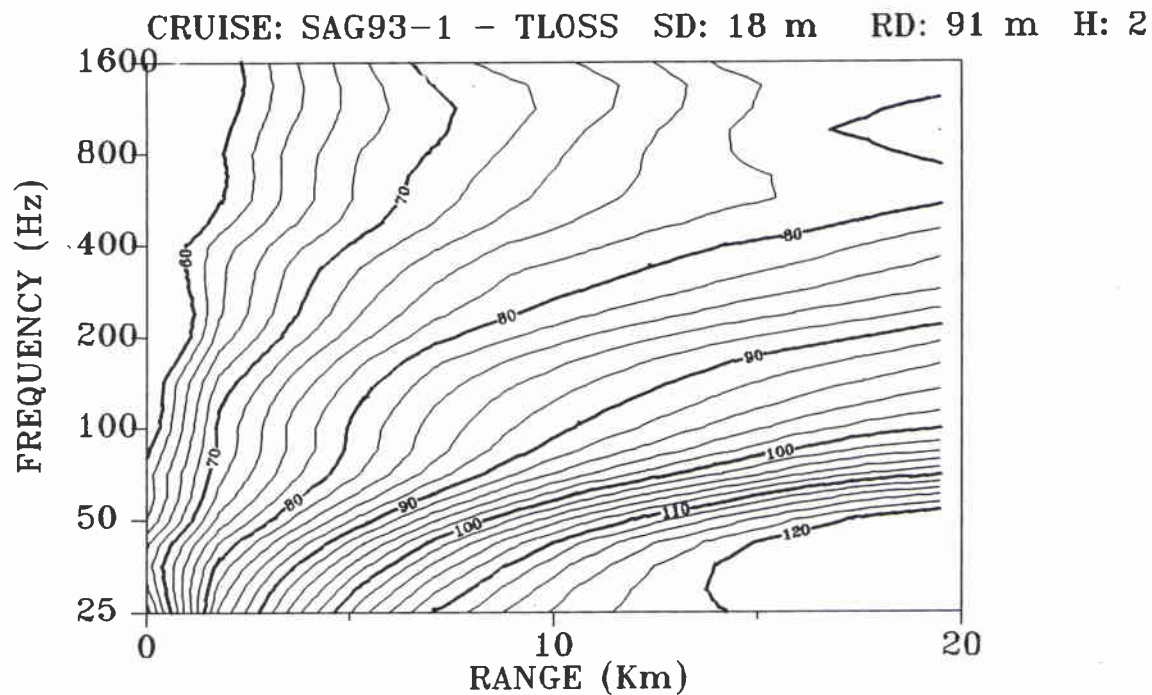
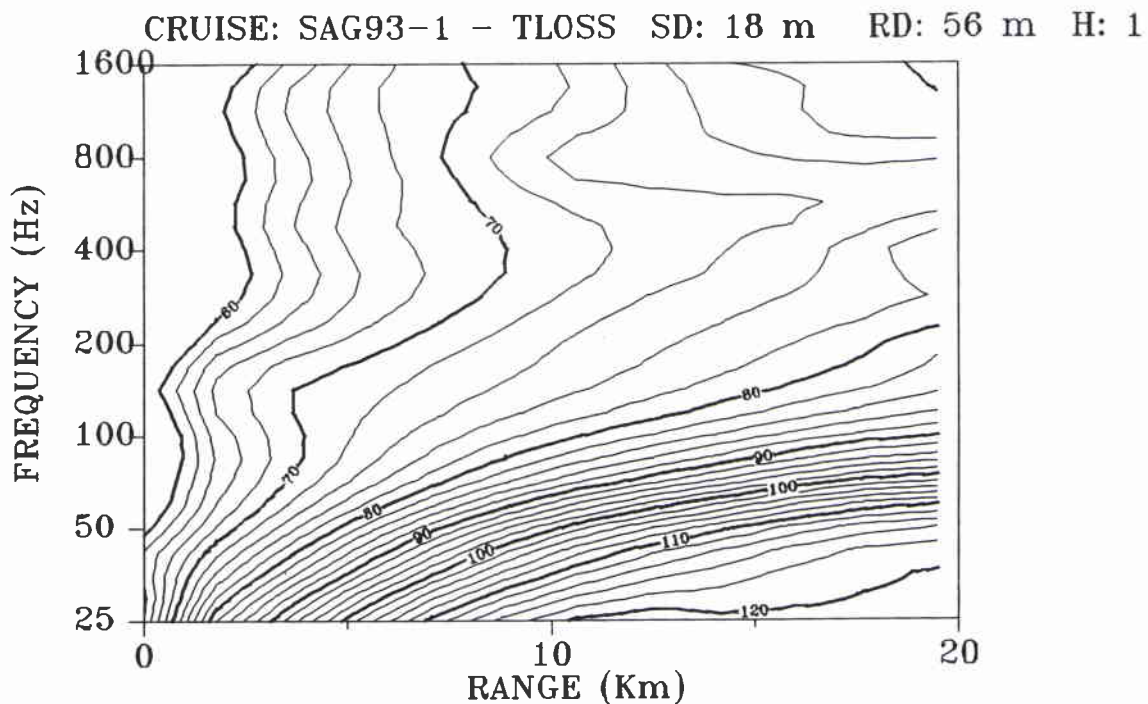


Figures 41–45 Transmission loss vs range. The circles are the measurements, processed in a 1/3 octave band. The solid line the SAFARI prediction using the high shear-velocity geoacoustic model of Table 4, while the dotted line is the SAFARI prediction using the low shear-velocity model of Table 3. SD=90 m; RD=91 m

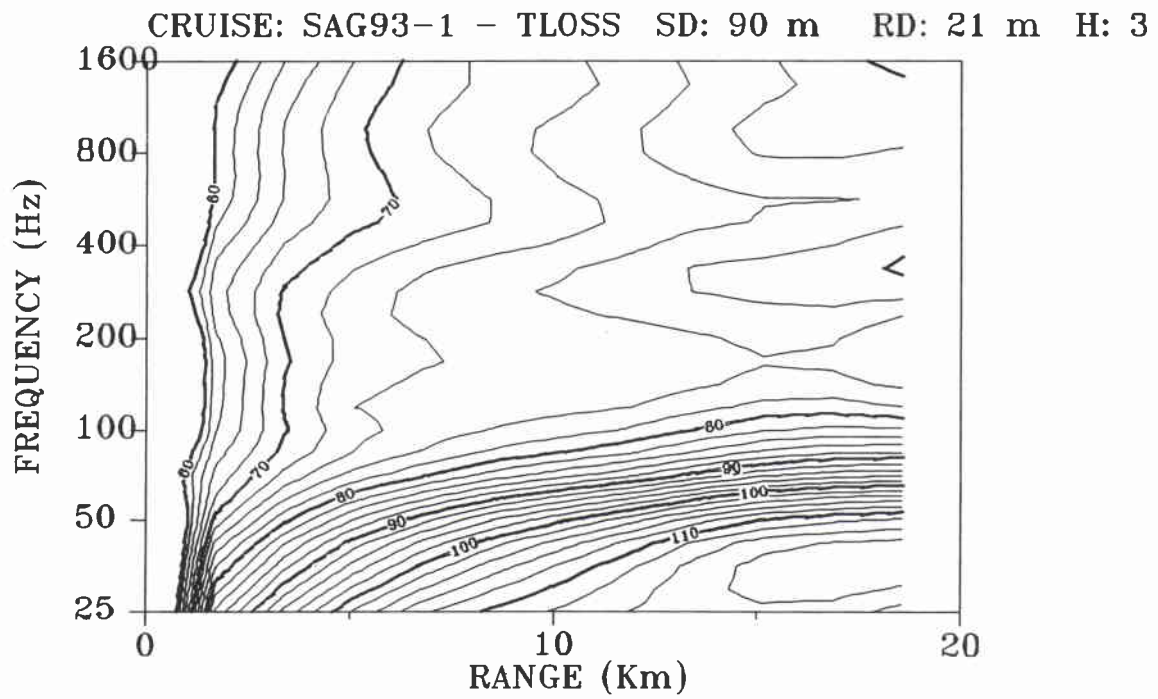
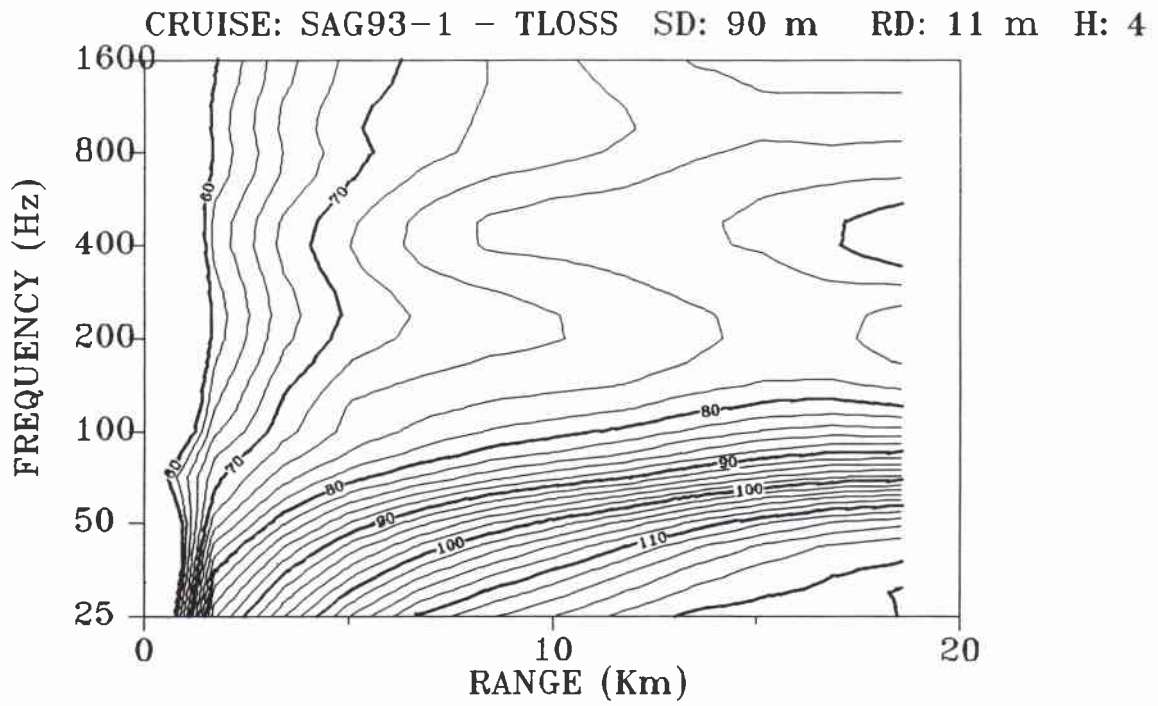


Figures 46-47 Transmission loss vs. frequency and range.

SACLANTCEN SR-243

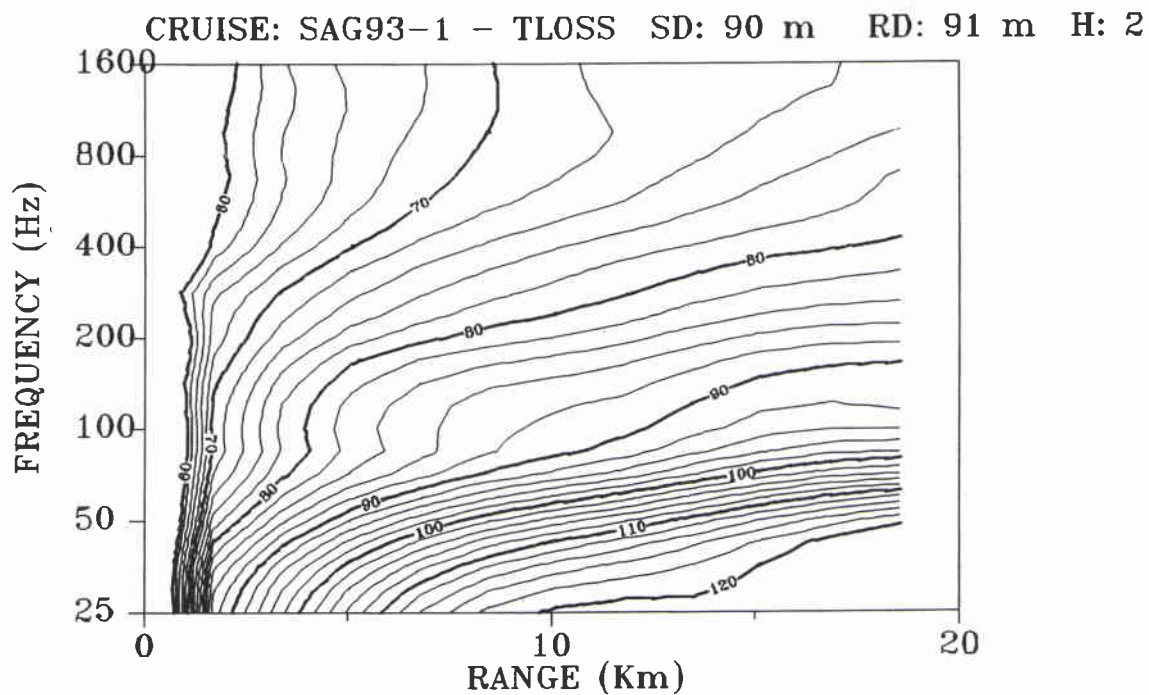
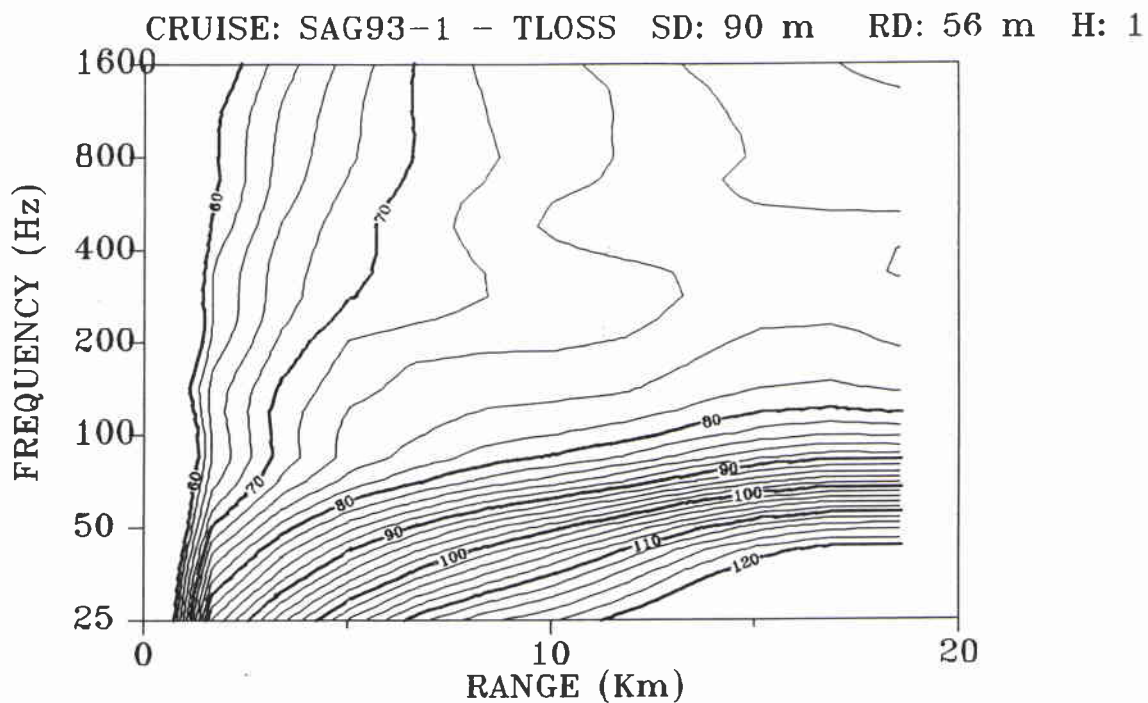


Figures 48-49 Transmission loss vs. frequency and range.



Figures 50-51 Transmission loss vs. frequency and range.

SACLANTCEN SR-243



Figures 52-53 Transmission loss vs. frequency and range.

Annex A

Particle motion of interface wave arrivals

In this annex we investigate the particle motion of the two possible interface-wave arrivals as recorded by the OBS. An interface wave of the Scholte type propagating in a laterally isotropic medium should exhibit particle motion only in the sagittal plane, while an interface wave of the Love type, under the same assumptions, would have motion only on the normal plane. To determine the particle motion in the radial (R), transverse (T), and vertical (V) directions with respect to wave propagation direction the signals on the three axis of the OBS were rotated, filtered, and integrated. The various stages of the processing are shown in Figs. A1–A3. This makes it possible to determine the particle orbits in the sagittal (R-V), normal (T-V) and horizontal (R-T) planes.

In Figs. A4–A8 the particle motion of Fig. A3 is projected on the horizontal, normal and sagittal planes in 2 second windows. It can be seen that, for every window, there is some energy in all the three planes. These data are somewhat similar to those reported by Macbeth [11] where the inability of distinguish a plane of motion was taken as an indication of anisotropy of the propagating medium. It should also be noted that the motion in the horizontal plane (which is incompatible with interface wave propagation) is at a minimum with respect to the motion in the other planes in the 6–8 second window, corresponding to the late arrival that was identified at the very beginning as the interface wave.

The particle motion analysis does not allow any definite conclusion about the nature of the waves recorded, but, the following observations can be made:

- a) there is a low-frequency late arrival that has most of the characteristics of an interface wave, with particle motion in the sagittal and normal plane. This arrival can be identified in almost all the time series recorded. The group velocity of this arrival is between 650–500 m/s in the 3–10 Hz frequency range, too low to be consistent with the estimated compressional-wave velocity;
- b) there is a low frequency arrival with group velocity of about 1000 m/s in the 6–9 Hz range, a velocity consistent with the estimated compressional-wave velocity, detectable only on the data recorded at the longest range. The particle motion of this arrival does not have the characteristics of an interface wave, but the fact that this arrival is embedded in other arrivals from reflected/refracted compressional waves, which cannot be completely eliminated by filtering, has to be taken into account;
- c) whether one or the other (or both) arrivals are any sort of interface wave, the contemporary motion on the sagittal and normal planes suggests a strong anisotropy of the medium. Under these conditions, the inversion technique (which assumes an isotropic medium) is liable to give incorrect results;
- d) if the 1000 m/s group velocity arrival is the interface wave, then the late low-frequency arrival needs to be explained. Computer simulations of the time series assuming a bottom model with the estimated compressional velocity and an shear

SACLANTCEN SR-243

velocity computed using the 1.9 compressional to shear velocity ratio do show an interface wave developing with about 1000 m/s group velocity, but do not show any evidence of a later arrival.

The discussion above shows that we were not able to reach a conclusion about the *in-situ* shear wave velocity in the Mallorca area. In particular, we found that the environment was of unexpected complexity for the estimation methods developed thus far, although the same methods gave successful results in several other locations. One possible line for future work is to design an experiment specifically aimed at resolving the ambiguities encountered in the Mallorca data, and in particular to address the anisotropy problem. Some studies on these lines, that may be taken as an indication of experimental design, have been reported by Snoek [12], although on a site with totally different bottom characteristics.

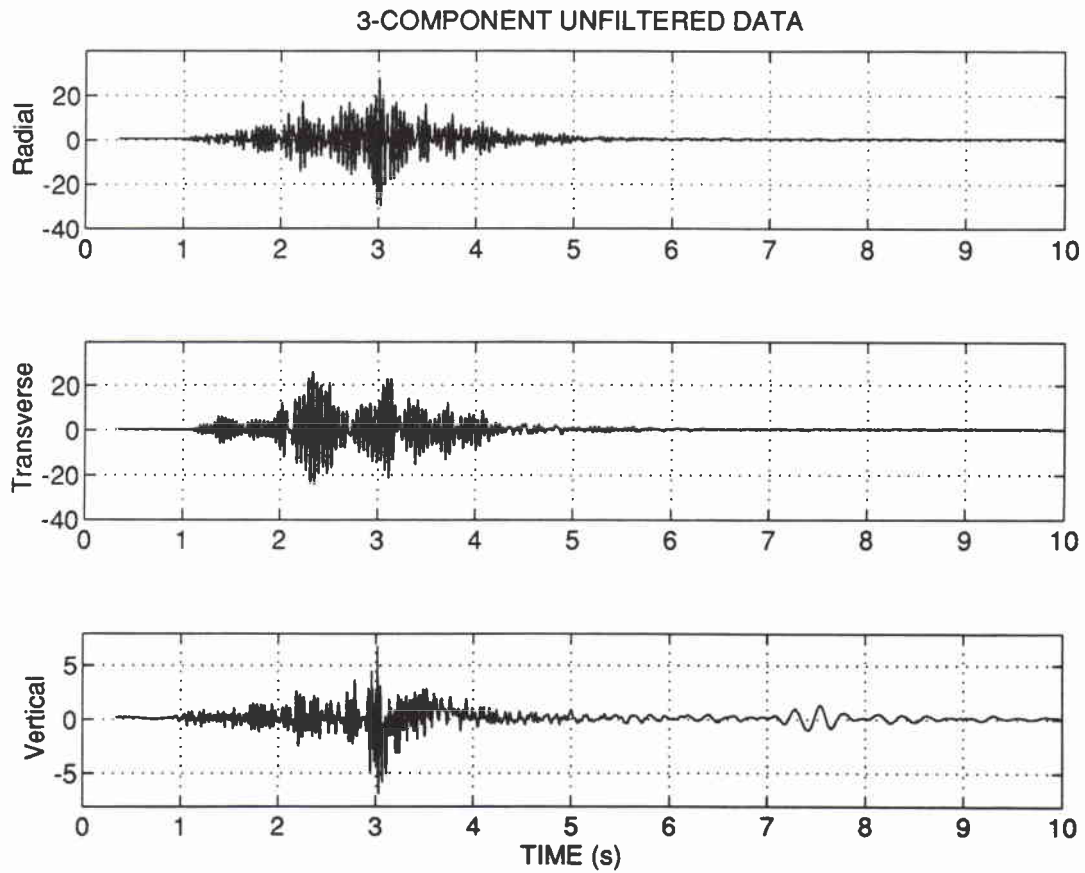


Figure A1 Normalized particle displacement (m/s ref. 1 @ 10 mV) vs. time (sec) measured by an OBS at a range of 4400 m from the explosive source. The data has been corrected so that the radial motion (R) is in the direction of the source, the transverse motion (T) is horizontal and perpendicular to the source direction, and the vertical motion (V) is perpendicular to the seabed.

SACLANTCEN SR-243

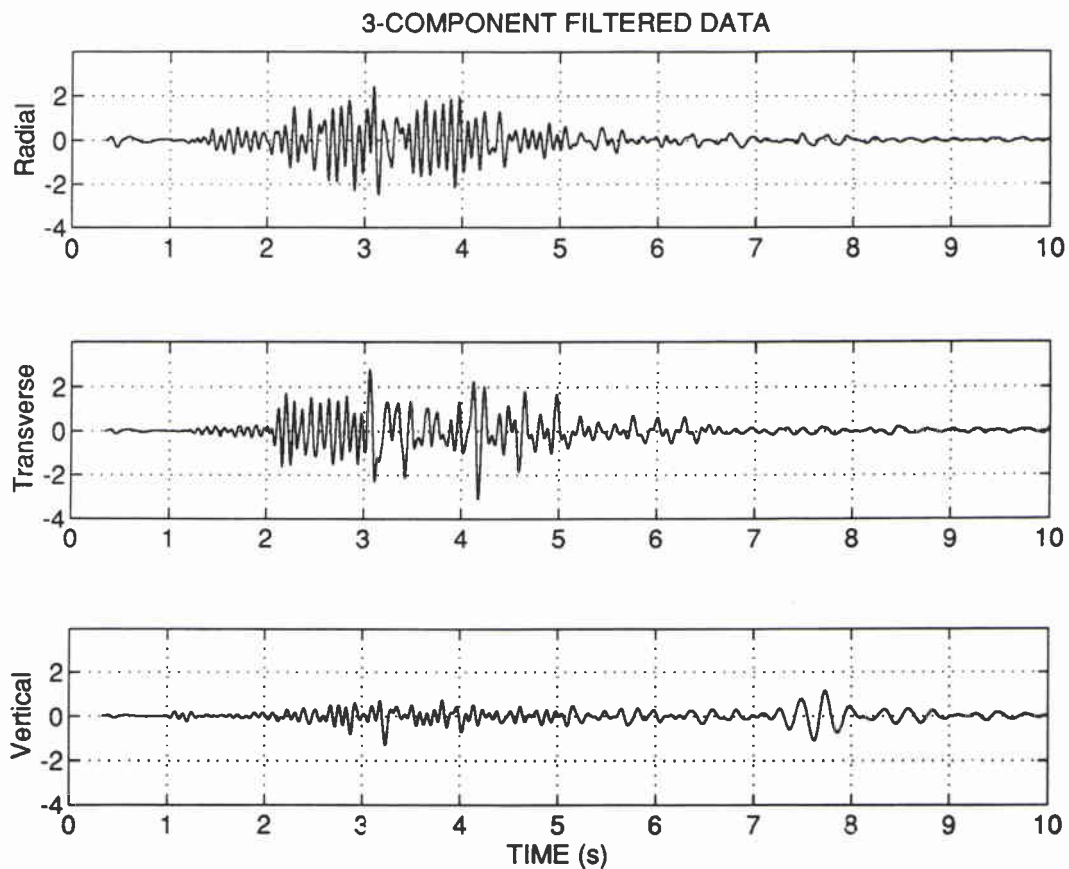


Figure A2 Same as *Figure A1* but low pass filtered.

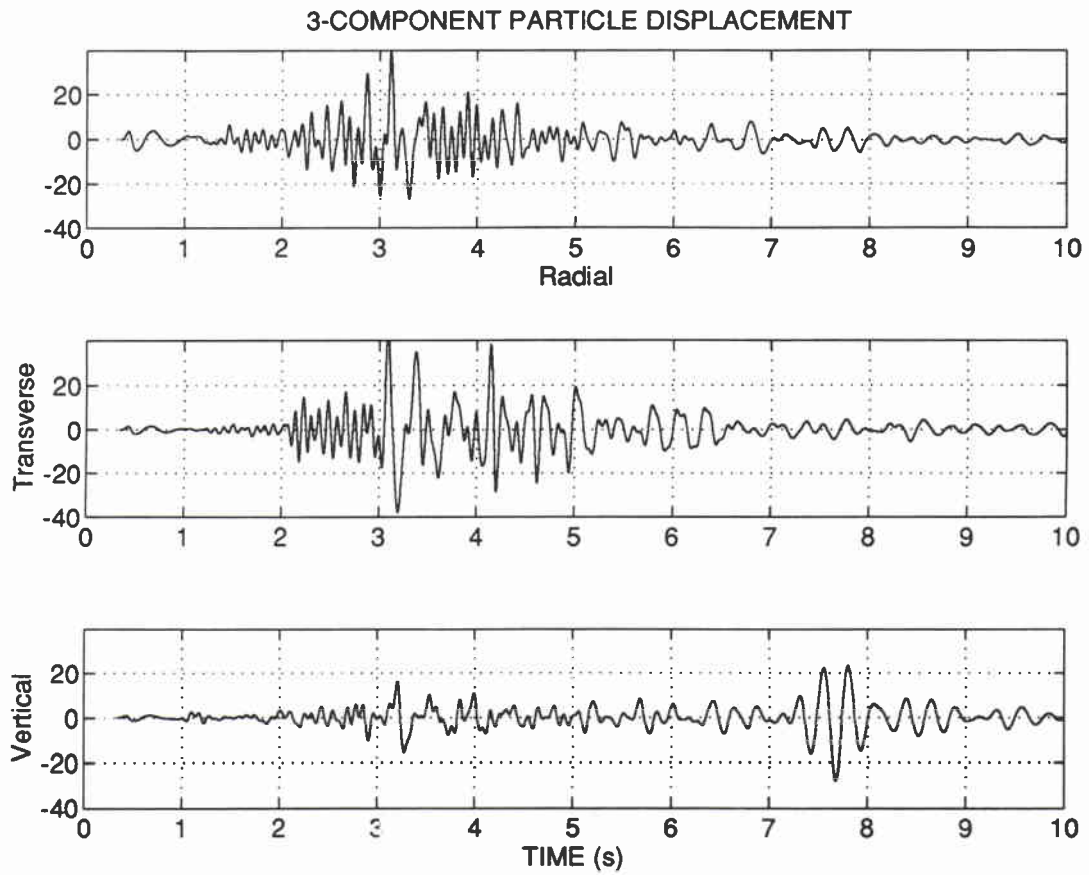


Figure A3 Normalized particle displacement in the interval is derived from the data of Figure A2.

SACLANTCEN SR-243

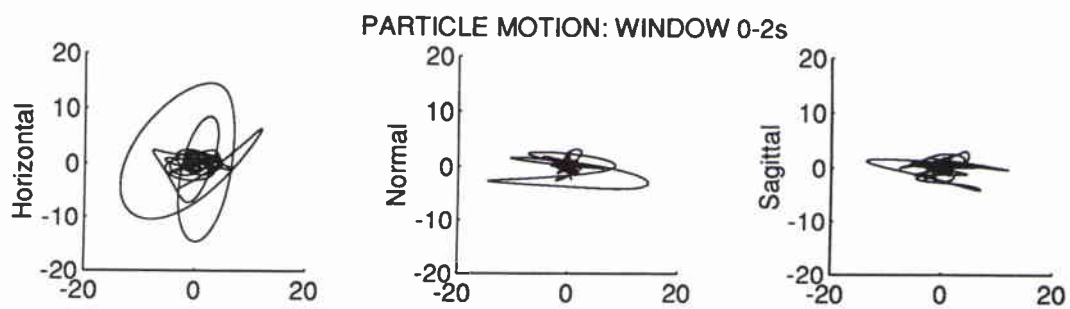


Figure A4 *The particle motion in the interval 0–2 s.*

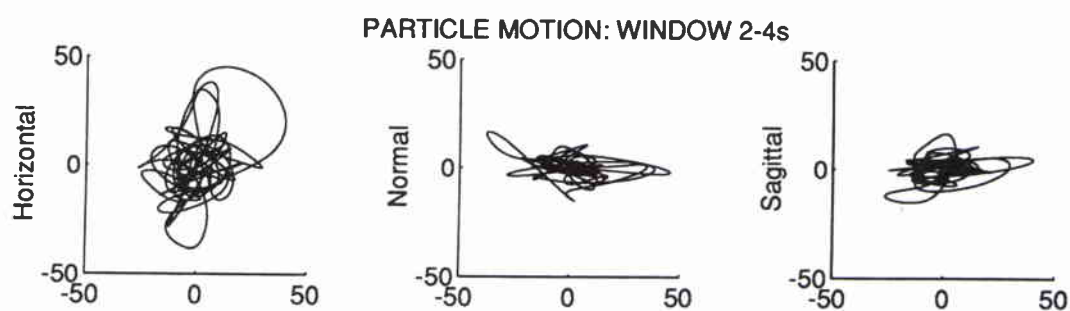


Figure A5 *The particle motion in the interval 2–4 s.*

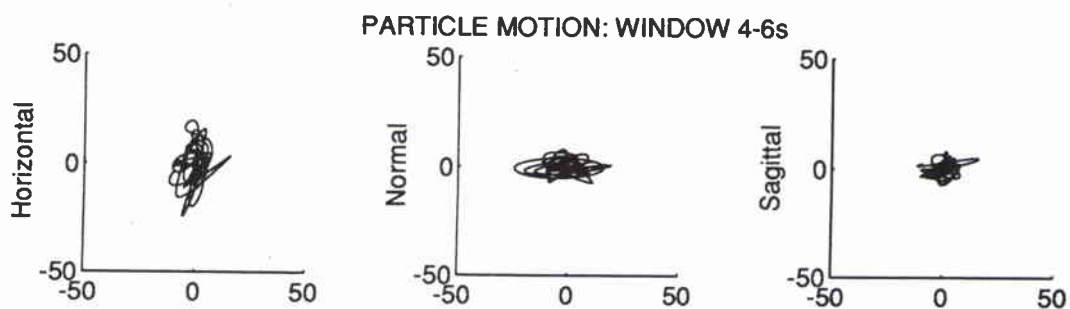


Figure A6 *The particle motion in the interval 4–6 s.*

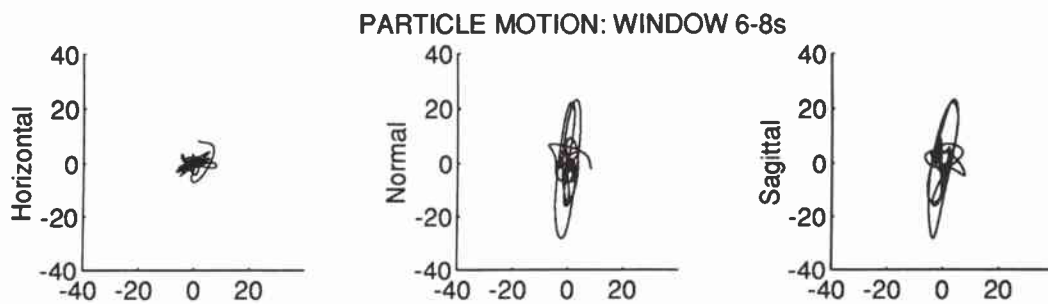


Figure A7 *The particle motion in the interval 6–8 s.*

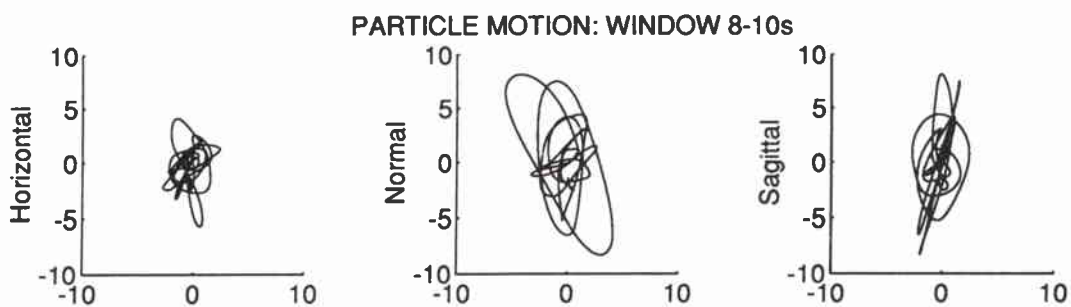


Figure A8 *The particle motion in the interval 8–10 s.*

Document Data Sheet

<i>Security Classification</i>		<i>Project No.</i>
		12
<i>Document Serial No.</i>	<i>Date of Issue</i>	<i>Total Pages</i>
SR-243	December 1995	44 pp.
<i>Author(s)</i>		
A. Caiti F. Ingenito, A. Kristensen and M. D. Max		
<i>Title</i>		
Acoustic bottom characterization of a shallow water area west of Mallorca		
<i>Abstract</i>		
<p>An experiment was conducted in shallow water on the Balearic Shelf west of the island of Mallorca. The seafloor in this area consists of a patchy layer of sediment less than 4 m thick overlying a hard limestone bottom. The compressional and shear velocities of the bottom were measured by remote sensing techniques using a geophone/hydrophone array deployed on the bottom and explosive sources. The compressional velocity in the basement was found to increase from 1970 m/s at the sediment-basement interface to 4305 m/s at a depth of 174 m. The shear velocity, determined from the inversion of interface wave data, was ambiguous, since there were two arrivals which could be interpreted as the interface wave. The slower arrival gave a shear velocity of about 600 m/s while the faster arrival gave a shear velocity of about 1100 m/s. Two geoacoustic models were constructed based on these results and used as inputs to SAFARI to predict transmission loss. Simultaneously with the bottom measurements, transmission loss was measured in a 100-1600 Hz band using explosive sources and a four element vertical array. At high frequencies (400, 800, 1600 Hz), in most cases, transmission loss predictions from both geoacoustic models compared reasonably well with the measurements, but at low frequencies (100, 200 Hz) the higher shear velocity model gave better agreement. The optimum frequency of propagation was about 800 Hz, higher than normally found in shallow water. This result is in agreement with theoretical predictions and is due to conversion to and subsequent absorption of shear waves in the bottom. It is suggested that the ambiguity in the determination of shear velocity could be due to anisotropy in the bottom.</p>		
<i>Keywords</i>		
Balearic Shelf – bottom characteristics – Mallorca – shallow-water		
<i>Issuing Organization</i>		
North Atlantic Treaty Organization SACLANT Undersea Research Centre Viale San Bartolomeo 400, 19138 La Spezia, Italy		Tel: +39 (0)187 540 111 Fax: +39 (0)187 524 600 E-mail: library@saclantc.nato.int
[From N. America: SACLANTCEN CMR-426 (New York) APO AE 09613]		

Initial Distribution for SR-243

Ministries of Defence

DND Canada	10
CHOD Denmark	8
DGA France	8
MOD Germany	15
HNDGS Greece	12
MARISTAT Italy	10
MOD (Navy) Netherlands	12
NDRE Norway	10
MDN Portugal	5
MOD Spain	2
TDKK Turkey	5
MOD UK	20
ONR US	49

NATO Authorities

NAMILCOM	2
SACLANT	3
CINCEASTLANT/	1
COMNAVNORTHWEST	1
CINCIBERLANT	1
CINCWESTLANT	1
COMASWSTRIKFOR	1
COMMAIREASTLANT	1
COMSTRIKFLTANT	1
COMSUBACLANT	1
SACLANTREPEUR	1
SACEUR	1
CINCNORTHWEST	2
CINCSOUTH	1
COMEDCENT	1
COMMARAIRMED	1
COMNAVSOUTH	1
COMSTRIKFOR SOUTH	1
COMSUBMED	1
SHAPE Technical Centre	1
PAT	1

SCNR for SACLANTCEN

SCNR Belgium	1
SCNR Canada	1
SCNR Denmark	1
SCNR Germany	1
SCNR Greece	1
SCNR Italy	1
SCNR Netherlands	1
SCNR Norway	1
SCNR Portugal	1
SCNR Spain	1
SCNR Turkey	1
SCNR UK	1
SCNR US	2
French Delegate	1
SECGEN Rep. SCNR	1
NAMILCOM Rep. SCNR	1

National Liaison Officers

NLO US	1
NLO Canada	1
NLO Denmark	1
NLO Germany	1
NLO Italy	1
NLO Netherlands	1
NLO UK	1

Total external distribution	212
SACLANTCEN Library	18
Total number of copies	230